Biochimica et Biophysica Acta 1817 (2012) 1646–1659

Contents lists available at SciVerse ScienceDirect

Biochimica et Biophysica Acta

journal homepage: www.elsevier.com/locate/bbabio

Thermodynamic constraints shape the structure of carbon fixation pathways

Arren Bar-Even, Avi Flamholz, Elad Noor, Ron Milo *

Department of Plant Sciences, The Weizmann Institute of Science, Rehovot 76100, Israel

ARTICLE INFO

Article history:
Received 27 March 2012
Received in revised form 7 May 2012
Accepted 9 May 2012
Available online 17 May 2012

Keywords:
Reduction potential
Carbon fixation
Thermodynamic favorability
Exergonism
Reaction coupling
ATP cost

ABSTRACT

Thermodynamics impose a major constraint on the structure of metabolic pathways. Here, we use carbon fixation pathways to demonstrate how thermodynamics shape the structure of pathways and determine the cellular resources they consume. We analyze the energetic profile of prototypical reactions and show that each reaction type displays a characteristic change in Gibbs energy. Specifically, although carbon fixation pathways display a considerable structural variability, they are all energetically constrained by two types of reactions: carboxylation and carboxyl reduction. In fact, all adenosine triphosphate (ATP) molecules consumed by carbon fixation pathways – with a single exception – are used, directly or indirectly, to power one of these unfavorable reactions. When an indirect coupling is employed, the energy released by ATP hydrolysis is used to establish another chemical bond with high energy of hydrolysis, *e.g.* a thioester. This bond is cleaved by a downstream enzyme to energize an unfavorable reaction. Notably, many pathways exhibit reduced ATP requirement as they couple unfavorable carboxylation or carboxyl reduction reactions to exergonic reactions other than ATP hydrolysis. In the most extreme example, the reductive acetyl coenzyme A (acetyl-CoA) pathway bypasses almost all ATP-consuming reactions. On the other hand, the reductive pentose phosphate pathway appears to be the least ATP-efficient because it is the only carbon fixation pathway that invests ATP in metabolic aims other than carboxylation and carboxyl reduction. Altogether, our analysis indicates that basic thermodynamic considerations accurately predict the resource investment required to support a metabolic pathway and further identifies biochemical mechanisms that can decrease this requirement.

1. Introduction

Central metabolic pathways have been subject to natural selection for many millions of years. As such, their structures can be viewed, in many cases, as solutions to evolutionary optimization problems. In this view, a given pathway can be explained, at least partially, by the selection pressures and constraints imposed on the optimization [1–6]. Thermodynamics impose one such constraint: all reactions in a pathway must be thermodynamically favorable under physiological conditions [7–9]. Here we focus on the effect of these energetic constraints on the structure of natural carbon fixation pathways and on the cellular resources they consume, specifically ATP [7,10–12].

Several carbon fixation pathways are currently known to support autotrophic growth [11,13,14]. The reductive pentose phosphate cycle (Fig. 1A), which operates in all photosynthetic eukaryotes and many prokaryotes, has been studied extensively [15–19]. The four acetyl-CoA–succinyl-CoA pathways (Fig. 1B) share a remarkable structural similarity but differ in their phylogenetic distribution, oxygen sensitivity, kinetic and thermodynamic profiles [11–14,20,21]. The reductive acetyl-CoA pathway and the glycine synthase pathway (Fig. 1C) directly reduce CO_2 and use the ubiquitous C1 carrier tetrahydrofolate (THF) to further metabolize the reduced C1 group [22–26]. However, the glycine synthase pathway is not used for autotrophic growth, but rather for the recycling of reduced electron carriers [12,27].

In recent studies we analyzed the thermodynamics of the net carbon fixation reaction of the various carbon fixation pathways and showed that their feasibility is dependent on several factors, including the number of ATP hydrolyzed, the reduction potential of electron carriers, the concentration of inorganic carbon, the cellular pH and the ionic strength [12,28]. Our analysis revealed that several carbon fixation pathways hydrolyze considerably more ATP molecules than required. For example, the reductive pentose phosphate pathway hydrolyzes 9 ATP molecules during the fixation of CO_2 to glyceraldehyde 3-phosphate, although 4–5 ATP molecules are sufficient to make the net reaction thermodynamically favorable. Similarly, most of the acetyl-CoA–succinyl-CoA pathways hydrolyze more ATP than would be expected from their net reactions. This excess ATP investment suggests that there might be local thermodynamic constraints that are ignored in analyzing only the net reaction.

On other hand, other carbon fixation pathways, *e.g.* the reductive acetyl-CoA pathway, operate at the thermodynamic edge and are favorable only in very specific conditions. In a sense, these pathways hydrolyze precisely the right number of ATP molecules required to achieve feasibility of their overall reaction, suggesting that at least some pathways are able to bypass the local thermodynamic constraints without extra ATP investment.

Abbreviations: $\Delta_r G'^m$, Transformed Gibbs energy of a reaction under reactant concentrations of 1 mM.

* Corresponding author. Tel.: +972 505714697; fax: +972 89344540.
E-mail address: ron.milo@weizmann.ac.il (R. Milo).

0005-2728
doi:10.1016/j.bbabio.2012.05.002

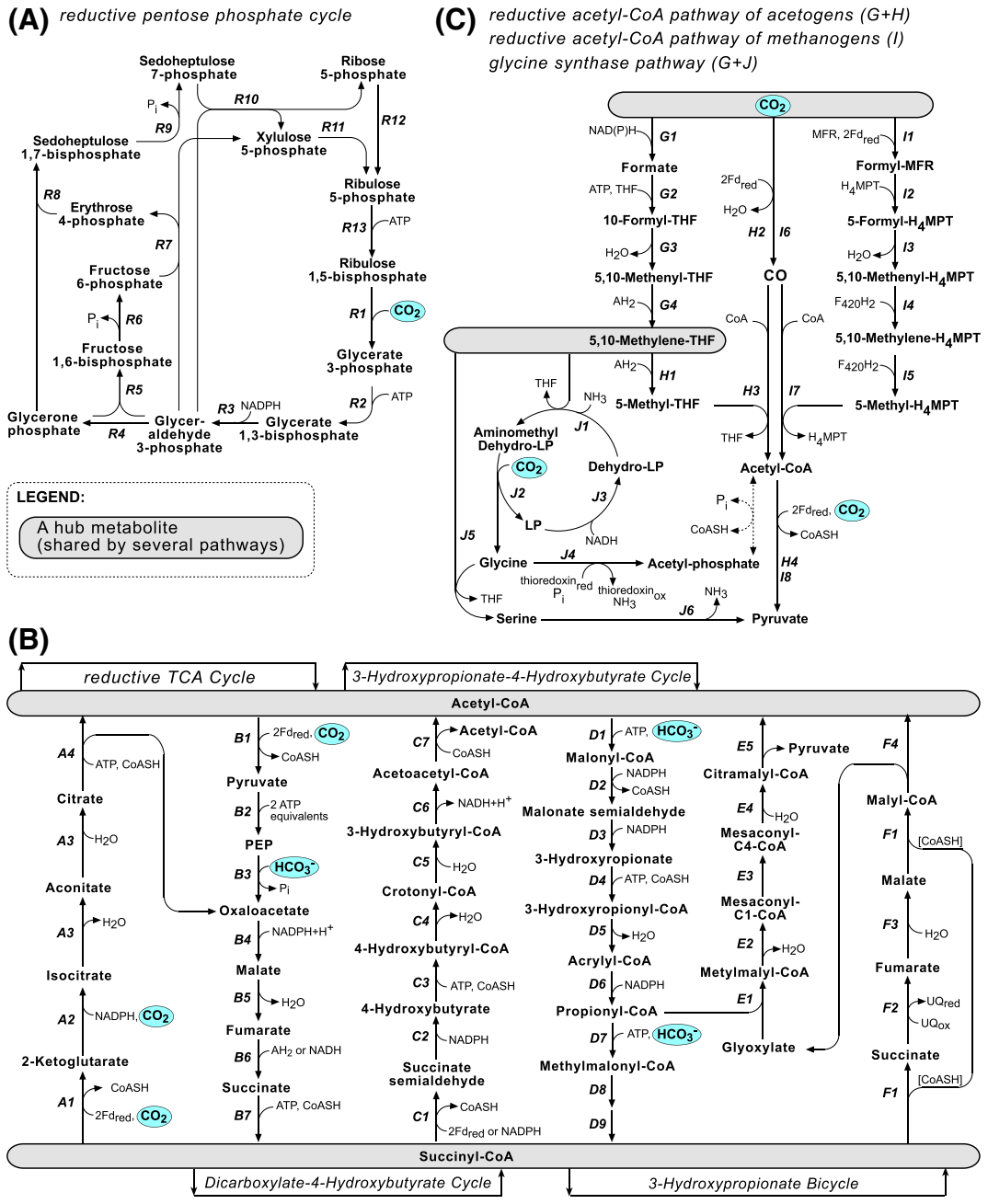

Fig. 1. The natural carbon fixation pathways currently known. (A) The reductive pentose phosphate pathway. (B) The four acetyl-CoA–succinyl-CoA carbon fixation pathways. (C) The C1 carbon fixation pathways. Hub metabolites, which are shared by several pathways, are marked with gray framing. Fd corresponds to ferredoxin and UQ to ubiquinone. 'AH_2' corresponds to a reduced electron donor, while 'A' represents an oxidized electron donor. THF corresponds to tetrahydrofolate, MPT to methanopterin, MFR to methanofuran and F_{420} to reduced deazaflavin factor 420. The glycine cleavage system is composed of the enzymes J1, J2 and J2, where 'LP' corresponds to lipoyl-protein (H-protein of the glycine cleavage system).Enzymes: (R1) Rubisco; (R2) Phosphoglycerate kinase; (R3) Glyceraldehyde-3-phosphate dehydrogenase (phosphorylating); (R4) Triose-phosphate isomerase; (R5) Fructose-bisphosphate aldolase; (R6) Fructose-bisphosphatase; (R7) Transketolase; (R8) Aldolase (Fructose-bisphosphate aldolase); (R9) Sedoheptulose-bisphosphatase; (R10) Transketolase; (R11) Ribose-5-phosphate isomerase; (R12) Ribulose-phosphate 3-epimerase; (R13) Phosphoribulokinase; (A1) 2-Ketoglutarate synthase; (A2) Isocitrate dehydrogenase; (A3) Aconitase; (A4) ATP citrate lyase; (B1) Pyruvate synthase; (B2) Pyruvate water dikinase; (B3) PEP carboxylase; (B4) Malate dehydrogenase; (B5) Fumarase; (B6) Fumarate reductase; (B7) Succinyl-CoA synthetase; (C1) Succinyl-CoA reductase; (C2) 4-Hydroxybutyrate dehydrogenase; (C3) 4-Hydroxybutyryl-CoA synthetase; (C4) 4-Hydroxybutyryl-CoA dehydratase; (C5) Enoyl-CoA hydratase (Crotonase); (C6) 3-Hydroxybutyryl-CoA dehydrogenase; (C7) Acetyl-CoA C-acyltransferase; (D1) Acetyl-CoA carboxylase; (D2) 3-Oxopropionate dehydrogenase (Malonyl-CoA reductase); (D3) 3-Hydroxypropionate dehydorgenase; (D4) 3-Hydroxypropionyl-CoA synthetase; (D5) 3-Hydroxypropionyl-CoA dehydratase; (D6) Acrylyl-CoA reductase; (D7) Propionyl-CoA Carboxylase; (D8) Methylmalonyl-CoA Epimerase; (D9) Methylmalonyl-CoA Mutase; (E1) Methylmalyl-CoA Lyase; (E2) Methylmalyl-CoA dehydratase; (E3) Mesaconyl-CoA C1-C4 CoA transferase; (E4) Mesaconyl-C4-CoA hydratase; (E5) Citramalyl-CoA lyase; (F1) Succinyl-CoA:malate CoA transferase; (F2) Succinate Dehydrogenase; (F3) Fumarase and (F4) Malyl-CoA Lyase; (G1) Formate dehydrogenase; (G2) Formate tetrahydrofolate ligase; (G3) Methenyltetrahydrofolate cyclohydrolase; (G4) Methylenetetrahydrofolate dehydrogenase; (H1) Methylenetetrahydrofolate reductase; (H2) CO dehydrogenase; (H3) Acetyl-CoA synthase; (H4) Pyruvate synthase; (I1) Formylmethanofuran dehydrogenase; (I2) Formyl-MFR:H_4MPT formyltransferase; (I3) Methenyl-H_4MPT cyclohydrolase; (I4) Methylene-H_4MPT dehydrogenase; (I5) Methylene-H_4MPT reductase; (I6) CO dehydrogenase; (I7) Acetyl-CoA synthase; (I8) Pyruvate synthase; (J1) Aminomethyl transferase; (J2) Glycine dehydrogenase; (J3) Dehydrolipoyl dehydrogenase; (J4) Glycine reductase; (J5) Serine hydroxymethyltransferase and (J6) Serine deaminase.

In this study we uncover these local thermodynamic constraints. We begin by analyzing the energetics of generalized reaction types and show that each reaction type displays a characteristic change in Gibbs energy. Specifically, we show that carboxylations and the reduction of carboxyls to carbonyls are the primary energetically challenging reactions involved in carbon fixation. Next, we show that all ATP molecules hydrolyzed by all carbon fixation pathways – with a single exception – are coupled directly or indirectly to carboxylation or carboxyl reduction reactions. Since the number of thermodynamically challenging reactions in each pathway is higher than the number of ATP molecules required to make the net reaction favorable, it is clear why many pathways hydrolyze more ATP than we would naively expect. Finally, we discuss various biochemical mechanisms used by some pathways to decrease their ATP requirement by coupling energetically challenging reactions to exergonic reactions other than ATP hydrolysis.

2. Methods

2.1. $\Delta_rG'^m$ and the reversibility of reactions

Δ_rG' is the transformed Gibbs energy of a chemical reaction at a specified pH (which is kept constant during the reaction) [29]. A reaction can proceed in the forward direction only if it is associated with a negative Δ_rG'. It is common to report the change in Gibbs energy as $\Delta_rG'^o$: the change in Gibbs energy under standard conditions where all reactants have 1 M concentrations [29]. However, to give a more realistic picture of the energetic constraints imposed on cells we prefer to use $\Delta_rG'^m$, the change in Gibbs energy under the more physiological reactant concentrations of 1 mM [30–33]. A reaction with a positive $\Delta_rG'^m$ can still carry flux in the forward direction if the concentrations of the substrates are kept sufficiently above the concentrations of the products such that the actual Δ_rG' is negative. However, the concentrations of intracellular metabolites are limited: they are rarely above 10 mM or below 1 μM [30,33]. Thus, if $\Delta_rG'^m$ is sufficiently large then the reactants must acquire non-physiological concentrations to make the reaction favorable.

Perhaps the most energetically challenging reaction in central metabolism is the oxidation of malate to oxaloacetate (using $NAD(P)^+$ as electron acceptor), which is characterized by a large positive $\Delta_rG'^m$ of roughly +30 kJ/mol (at pH 7). It is useful to note that an order-of-magnitude difference between product and substrate concentrations decreases Δ_rG' by 5.7 kJ/mol. Hence, assuming that the concentration ratio $[NAD^+]/[NADH]$ is roughly 10, we find malate oxidation to be favorable only if [malate] ~10 mM and [oxaloacetate] ~1 μM, which is at the boundary of the physiological range of metabolite concentrations. Therefore, as a rule of thumb, we consider reactions with $\Delta_rG'^m > +30$ kJ/mol infeasible, requiring activation through coupling to exergonic reactions like ATP hydrolysis in order to sustain forward flux.

2.2. Calculation of $\Delta_rG'^m$ and E′ values

$\Delta_rG'^m$ values were calculated in one of the following ways: (1) $\Delta_rG'^m = \sum s_i \Delta_fG'_i$ where $\Delta_fG'_i$ is the transformed Gibbs energy of formation of reactant i and s_i is the stoichiometry of reactant i in the reaction. (The transformed Gibbs energy of the formation of a compound is the change in Gibbs energy during the formation of 1 mol of compound from its component elements at their standard state and at specified pH.) Calculations were done using eQuilibrator, the biochemical thermodynamics calculator, http://equilibrator.weizmann.ac.il/ [34]. (2) $\Delta_rG'^0 = RT\ln(K')$, where K′ values are experimentally derived equilibrium constants given in the comprehensive NIST Database of Thermodynamics of Enzyme-Catalyzed Reactions, http://xpdb.nist.gov/enzyme_thermodynamics/, [35]. In both cases $\Delta_rG'^m$ values were corrected to pH 7 and ionic strength of 0.1 M [36,37]. Reduction potentials, E′, were calculated from the $\Delta_rG'^m$ values of the half reactions. Only experimentally derived Δ_fG' values, taken from [36,38], were used to calculate E′. These values, along with their grouping into generalized reaction types are given in Appendix 1.

In specific cases (described in figure legends), when a required Δ_fG' value was not available experimentally, it was estimated by applying group contribution methodologies [39]. $\Delta_rG'^m$ values for reactions containing THF and H-protein were taken from [40,41] and the NIST database. All $\Delta_rG'^m$ values that were not calculated directly from experimentally derived Δ_fG' values were linearly optimized to fit the $\Delta_rG'^m$ of the overall pathway reactions. Δ_fG' for aqueous CO_2 was calculated considering all hydrated and unhydrated forms of the molecules (CO_2(aq), H_2CO_3(aq), HCO_3^-(aq), CO_3^{2-}(aq)) [36].

2.3. The reduction potential of the electron donors used by the carbon fixation pathways

The primary electron carriers used in carbon fixation pathways are NADPH and ferredoxin. The standard reduction potential of NADPH (a two electron carrier) is $E'^o = -320$ mV. Since the NADPH/$NADP^+$ ratio usually lies between 0.1 and 10 [30,42–45], we approximate E′ of NADPH (at pH 7) to lie in the -320 ± 30 mV range. Unlike NADPH, ferredoxin (a one electron carrier) comes in many forms, each characterized by a different reduction potential [46]. However, since the well studied Fe_2S_2 ferredoxin (from spinach) and Fe_4S_4 ferredoxin (from *Clostridium pasteurianum*) both have $E'^o = -420$ mV we use this value as a characteristic reduction potential for ferredoxin. Assuming again that the Fd^{red}/Fd^{ox} ratio lies between 0.1 and 10, the ferredoxin potential range is -420 ± 60 mV.

2.4. pH dependence of the reduction potential

Changes in pH can significantly affect the reduction potential. This is because protons are added to the reduced molecule alongside electrons (for example, in the reduction of acetaldehyde to ethanol by two electrons, two protons also join the molecule). The dependence of the reduction potential on pH is a direct function of the ratio between the number of protons and electrons that join the molecule upon its reduction. If every electron is accompanied by a single proton, the pH-dependent change in reduction potential is $-RT\cdot\ln(10)/F \sim -60$ mV per pH unit.

Since the reduction of hydroxycarbons and carbonyls corresponds to the addition of two electrons and two protons, the pH-dependent change is ~−60 mV per pH unit. The reduction of carboxyls (whose pKa is significantly lower than 6) is characterized by a reduction potential change of ~−90 mV/pH, corresponding to the addition of three protons per reduction with two electrons. Notably, if the molecule being reduced contains an ionizable group with a pKa value close to pH 6–8 (*e.g.* phosphate groups), change in the pH will also affect the protonation state of these groups, resulting in a further modulation of the reduction potential. Since hydrated CO_2 has a pKa value near 7, the pH dependence of the reduction potential of CO_2 to formate or CO is not an integer multiple of −30 mV per pH unit.

As the reduction of $NADP^+$ involves the addition of one proton per two electrons, its reduction potential changes by ~−30 mV per pH unit. The dependence of ferredoxin's reduction potential on pH is different for different ferredoxin variants [47]. However, since this dependence is usually small and since both the Fe_2S_2 ferredoxin from spinach and the Fe_4S_4 ferredoxin from *Clostridium pasteurianum* were found to be pH independent [48–50] we approximate ferredoxin's reduction potential to be pH independent.

3. Results

3.1. Generalized reaction types display characteristic energetic profiles

The change in Gibbs energy due to a reaction might be specific, dependent on the exact identity of the substrates and products. If this is the case, identifying the thermodynamic barriers in a pathway will

require a careful, independent analysis of each reaction. However, reactions of the same type (*e.g.* alcohol dehydrogenases) may exhibit similar energetic profiles. If indeed the reaction Gibbs energy is determined mostly by its type, the thermodynamically limiting reactions in a pathway could be identified through a quick survey of the reaction types involved.

To analyze whether a reaction's type is the major determinant of its energetics we focused on oxidoreductase reactions. We used experimentally measured equilibrium constants (K′) taken from the NIST database of thermodynamics of enzyme-catalyzed reactions [35] as well as experimentally derived Gibbs energies of formation ($\Delta_f G'$) [34,36,38] to calculate the reduction potential of all possible half-reactions (Methods and Appendix 1). For simplicity, only compounds composed of carbon, oxygen and hydrogen were considered. We then grouped the half-reactions according to the functional group being reduced. Three such groups were defined as follows: reactions in which a carboxyl (–COOH) is reduced to a carbonyl (–CO–), reactions in which a carbonyl is reduced to a hydroxycarbon (–CHOH–) and reactions in which a hydroxycarbon is reduced to a hydrocarbon ($-CH_2-$) (the reduction of a hydroxycarbon to a hydrocarbon take place through an alkene intermediate). Two additional reactions – CO_2 reduction to formic acid and to carbon monoxide – are treated individually.

Fig. 2 shows the distribution of reduction potentials (marked with horizontal lines) and their clustering into generalized groups (the color of the horizontal lines and surrounding boxes). The distributions of reduction potentials within the groups are quite wide (>100 mV), suggesting that the chemical environment surrounding a functional group can significantly affect its reduction potential. However, Fig. 2 also demonstrates that the generalized groups are well separated in their reduction potentials and, thus, the oxidation state of a carbon is the major determinant of its reduction potential. While a previous study has shown that the *average* reduction potentials of these groups are different [32], to the best of our knowledge this is the first time a systematic analysis demonstrates that the reduction potential ranges of the different groups are well-separated in aqueous conditions.

As previously suggested [32], we find that more reduced carbons (having low oxidation state) have higher reduction potentials, *i.e.* have a greater tendency to accept electrons. Hence, when electrons are donated by a functional group at higher oxidation state (relatively oxidized carbon) to a functional group at lower oxidation state (relatively reduced carbon), energy is released. On the other hand, the reduction of a group at higher oxidation state by a group at lower oxidation state should be coupled to an exergonic reaction for it to become thermodynamically favorable. A major exception to the general reduction potential trend is the reduction potential of CO_2 to formic acid, which is higher than that of carboxyls to carbonyls (Fig. 2).

The general trend in reduction potential suggests that a basic knowledge of the reaction types involved in a pathway provides enough information to infer which reactions will be thermodynamic barriers. Specially, we can analyze the feasibility and reversibility of different oxidoredcutase reactions according to the trend. As a rule of thumb we consider reactions with $\Delta_r G'^m < -30$ kJ/mol to be irreversible and reactions with $\Delta_r G'^m > +30$ kJ/mol to be infeasible within the physiological range of metabolite concentrations (Methods); $\Delta_r G'^m$ being the transformed Gibbs energy of a reaction under reactant concentrations of 1 mM (Methods). For example, the reduction potentials of the main electron carriers used in carbon fixation pathways, NADP and ferredoxin (-320 ± 30 and -420 ± 60 mV, respectively, see Methods), are higher than the reduction potential of carboxyls to carbonyls (-600 mV $< E'^0 <$ -480 mV, Fig. 2). Hence, the reduction of a carboxyl to a carbonyl using NADPH as an electron donor is always thermodynamically infeasible ($\Delta_r G'^m > +30$ kJ/mol) without activation. Ferredoxin, which has a lower reduction potential, can serve as an electron donor for such a reduction only if the carboxyl being reduced has a relatively high reduction potential (such that the reduction potential difference between the electron donor and acceptor is relatively small and hence $\Delta_r G'^m$ less than +30 kJ/mol).

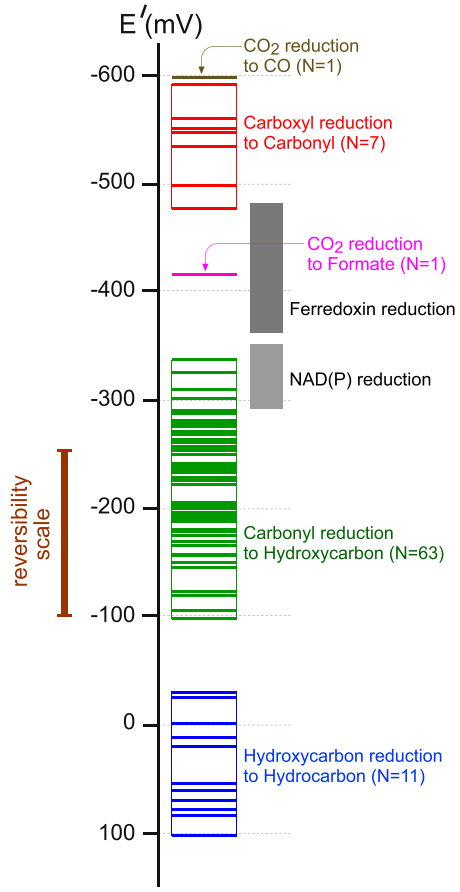

Fig. 2. The reduction potentials, E'^0, of electron carriers and half-reactions, at pH 7. E'^0 values were calculated using experimentally measured equilibrium constants (K′) and experimentally derived Gibbs energies of formation ($\Delta_f G'$) as described in the main text and in the Methods section. Values were corrected to pH 7 and ionic strength of 0.1 M and are given in Appendix 1. The reduction potentials are marked with horizontal lines. We grouped the reactions according to the specific functional group that is reduced. The colors of the horizontal lines correspond to the generalized group the reaction belongs to. While the reduction potentials of these generalized redox reactions depend on the specific molecules containing the functional groups, the figure shows that reactions in which the same functional group is reduced have similar reduction potentials. The light gray range corresponds to the reduction potential of NADH assuming that [NADH]/[NAD^+] ranges between 0.1 to 10. The dark gray range corresponds to the reduction potential of ferredoxin assuming that [$ferredoxin_{red}$]/[$ferredoxin_{ox}$] ranges between 0.1 to 10 (Methods). The vertical maroon / dark red bar represents the difference in reduction potentials between half-reactions which leads to a reversible electron transfer (assuming transfer of two electrons; $\Delta_r G'^m = 30$ kJ/mol).

The reduction potential of carbonyls to hydroxycarbons (-360 mV $< E'^0 < -100$ mV, Fig. 2) is higher than that of NAD(P)H or ferredoxin, meaning that using NAD(P)H or ferredoxin as electron donors in this reduction releases energy and is sometimes irreversible. The reduction potential of hydroxycarbons to hydrocarbons is so high (-40 mV $< E'^0 < 100$ mV at pH 7) that up to 100 kJ/mol are released by the irreversible reduction of a hydroxycarbon to a hydrocarbon using NADPH or ferredoxin as electron donors.

The general trend shown in Fig. 2 also affects the energetics of reactions that form or cleave a carbon–carbon bond. In fact, the formation (or cleavage) of a carbon–carbon bond is effectively an electron transfer reaction, where one carbon is reduced and the other is oxidized [32]. According to the general trend shown in Fig. 2 we expect the energetics of the condensation reaction to be more favorable if the carbon being reduced has a lower oxidation state (relatively reduced). As Fig. 3 depicts, the oxidation state of the carbon being reduced is the primary determinant of the energetics of the condensation reaction and the overall trend fits that of Fig. 2. Specifically, the formation of a carbon–carbon bond in which CO_2 or a carboxyl are reduced is infeasible without

external activation. On the other hand, the formation of a carbon–carbon bond in which a carbonyl is reduced to a hydroxycarbon (*i.e.* aldolase reactions) is readily reversible ($|\Delta_rG'^m|<20$ kJ/mol). Finally, the reduction and condensation of a hydroxycarbon with another carbon is occasionally irreversible.

3.2. Carboxylations and carboxyl reductions are the thermodynamic bottlenecks of the carbon fixation pathways

Focusing on carbon fixation pathways, we now ask which reaction types are expected to energetically constrain the process. We assume that all pathway reactions take place in one compartment, such that transport of intermediates across membranes does not impose or alleviate any energetic barriers. Carbon fixation pathways operate numerous oxidoreductase and carbon–carbon formation/cleavage reactions. According to the analysis presented above we can infer which of these reactions will likely impose an energetic barrier. First, as carbon fixation is basically a reductive process, the main oxidoreductase reaction type that is expected to challenge the process is carboxyl reduction using NADH or ferredoxin as electron donors. Moreover, since all carbon fixation pathways (with the exception of the reductive acetyl-CoA pathway) use carboxylation reactions to incorporate inorganic carbon, we expect carboxylation reactions to thermodynamically challenge most of them. While most carbon fixation pathways also cleave at least one carbon–carbon bond, this reaction is not expected to present a thermodynamic difficulty since the cleavage reaction can be performed such that a hydroxycarbon is oxidized to a carbonyl or a carbonyl is oxidized to a carboxyl; both of these reaction types are energetically favorable (Fig. 3).

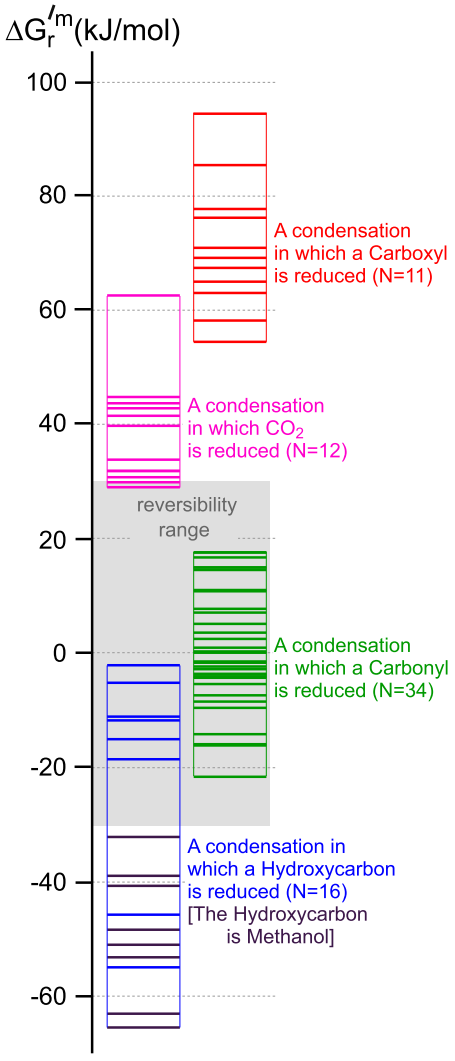

Fig. 3. Change in Gibbs energy under reactant concentrations of 1 mM, $\Delta_rG'^m$, for condensation reactions of functional groups composed of only carbon, oxygen and hydrogen, at pH 7. $\Delta_rG'^m$ values were calculated using experimentally measured equilibrium constants (K′) and experimentally derived Gibbs energies of formation (Δ_fG') as described in the main text and in the methods section. Values were corrected to pH 7 and ionic strength of 0.1 M and are given in Appendix 1. The $\Delta_rG'^m$ values of these reactions are marked with horizontal lines. We grouped the reactions according to the oxidation state of the carbon being reduced during the condensation reaction. The colors of the horizontal lines correspond to the generalized group the reaction belongs to. The purple lines correspond to a sub-group within the hydroxycarbon condensation reactions group: the condensation of methanol with another molecule. The gray range represents reversible reactions.

To test whether our estimations are correct we analyzed the core reaction steps of each of the carbon fixation pathways. Fig. 4 shows a schematic representation of all pathways, highlighting the major oxidoreductase and carbon–carbon bond formation/cleavage reactions. All ATP-hydrolyzing steps as well as substitutions of the carbon backbone (with CoA or THF, for example) are omitted. The $\Delta_rG'^m$ values of these reactions were calculated from the Gibbs energies of formation (Δ_fG') of the reactants (Methods) [34]. This stripped down representation reveals the underlying structure of the pathways and shows clearly which reactions are energetically challenging. Notably, as expected, all reactions requiring energetic activation ($\Delta_rG'^m \geq 30$ kJ/mol, shaded in red) are either carboxylations or carboxyl reductions. The reduction of CO_2 to carbon monoxide is the only thermodynamically challenging reaction in any carbon fixation pathway other than a carboxyl reduction or carboxylation (Fig. 4C).

In order to produce a given final product (*e.g.* pyruvate) via a non-C1 carbon fixation pathway, a fixed number of carboxylation and carboxyl reduction reactions are required regardless the path taken. For example, three carboxylations are required to produce pyruvate from CO_2. In addition, reducing CO_2 to pyruvate requires five reduction reactions, two of which are carboxyl reductions: two of the fixed CO_2 molecules within pyruvate are reduced while the third one remains a carboxylic acid. Together, one would expect the production of pyruvate to pass through five unfavorable reactions. However, a close inspection of Fig. 4B shows that some pathways reduce more than three carboxyls during pyruvate formation. The extra carboxyl reductions take place because some pathways also contain the reverse reaction: the oxidation of a carbonyl to a carboxyl. For example, four carboxyl reduction reactions are required to produce pyruvate in the dicarboxylate-4-hydroxybutyrate cycle because the cleavage of acetoacetate into two acetate molecules involves the oxidation of a carbonyl moiety to a carboxyl (Fig. 4B). An extra carboxyl reduction reaction is therefore required to compensate for the formation of the new carboxyl.

3.3. ATP investments in the carbon fixation pathways are coupled directly or indirectly to carboxylations or carboxyl reductions

Metabolic ATP investment is required primarily to activate otherwise infeasible biochemical transformations. If indeed carboxylation and carboxyl reduction constitute the only thermodynamic barriers to carbon fixation, we would expect all the ATP hydrolysis reactions to be coupled, directly or indirectly to one of these unfavorable reactions. Indeed, as shown in Table 1, we find that, with the exception of the reductive pentose phosphate pathway, the ATP hydrolysis reactions in all carbon fixation pathways are coupled either to carboxylation or carboxyl reduction.

Focusing on the acetyl-CoA–succinyl-CoA pathways, Fig. 5 shows that each hydrolyzed ATP is coupled to carboxyl reduction, carboxylation or both. The number of reaction steps between the ATP hydrolyzing reaction and the activated reaction is listed next to the arrow together with the temporary energy carrier used. For example, ATP hydrolysis by propionyl-CoA carboxylase is directly coupled to the carboxylation of propionyl-CoA by the same enzyme (Fig. 6A and reaction 'D7' in Fig. 1B). In other cases, ATP is hydrolyzed upstream of the reaction it actually activates and the energy of ATP hydrolysis is temporarily stored in a bond with high-energy of hydrolysis (a thioester, phosphoenol, etc.).

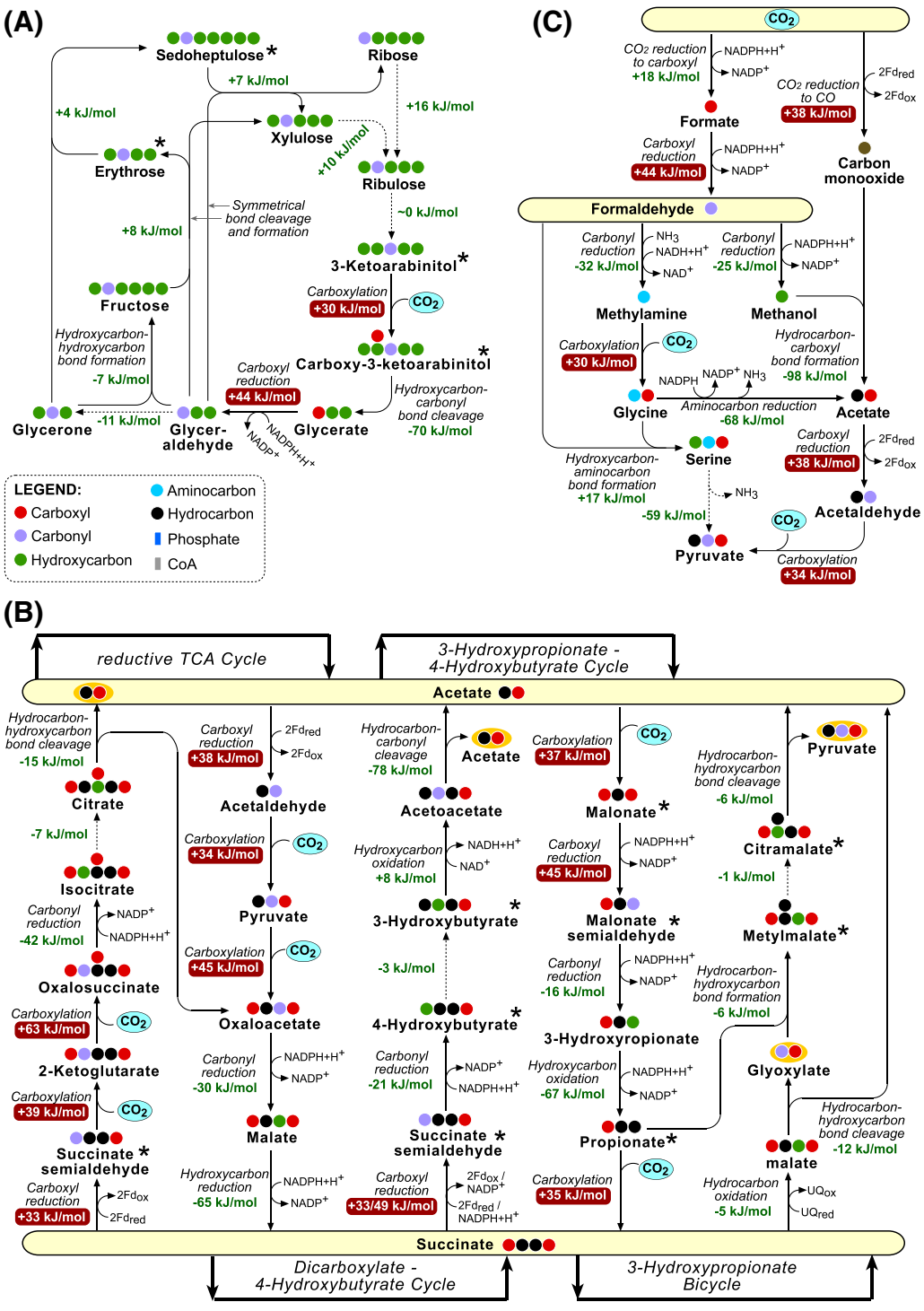

Fig. 4. A schematic representation of the metabolic backbone of the carbon fixation pathways. (A) The reductive pentose phosphate pathway; (B) the acetyl-CoA–succinyl-CoA pathways and (C) the C1 carbon fixation pathways. The figure displays only the oxidoreductase and carbon–carbon bond formation/clevage reactions of the pathways. All other reactions, including ATP hydrolysis, substitution with CoA, hydration and dehydration are not shown. Every circle corresponds to a carbon atom. We use a color notation scheme to display the different functional groups composing the metabolites, which also corresponds to the oxidation states of the carbons: red indicates a carboxyl, purple corresponds to a carbonyl, green to a hydroxylcarbon and black to a hydrocarbon. Fd corresponds to ferredoxin and UQ to ubiquinone. Changes in Gibbs energy under reactant concentrations of 1 mM, $\Delta_r G'^m$, are shown for all reactions. These values were calculated using eQuilibrator [34]. $\Delta_f G'$ values for compounds marked with "*" were calculated using group contribution [39]. All other $\Delta G_f'$ values were experimentally derived [36,38]. Notably, all reactions that require energetic activation ($\Delta_r G'^m \geq 30$ kJ/mol) are either carboxylation or carboxyl reduction, with the exception of CO_2 reduction to CO.

Consider the example of succinyl-CoA reductase (reaction 'C1' in Fig. 1B). The direct reduction of succinate to succinate semialdehyde is unfavorable ($\Delta_r G'^m = +33$–49 kJ/mol, depending on the electron donor, Fig. 4), as expected for the reduction of a carboxyl to a carbonyl. This reaction is activated by hydrolyzing the thioester bond between succinate and CoA, making the reduction of succinyl-CoA to succinate semialdehyde energetically favorable (Fig. 6B). However, forming a thioester bond requires energy input, which comes from ATP hydrolysis. In the dicarboxylate-4-hydroxybutyrate cycle the enzyme succinyl-CoA synthetase (enzyme 'B7' in Fig. 1B) couples ATP hydrolysis with the synthesis of succinyl-CoA. Therefore, the ATP hydrolyzed in reaction 'B7' should be regarded as an ATP investment needed to energize the

Table 1
Linkage between ATP hydrolyzing reactions and the unfavorable reactions they energizes.

Pathway	ATP investment aim	Reaction in which ATP is hydrolyzed‡	Number of ATP equivalents invested for the synthesis of pyruvate	Reaction that was energized by the ATP hydrolyzed‡
Reductive pentose phosphate pathway				
	Carboxyl reduction	Glycerate-3P kinase (R2)	5	Glyceraldehyde-3P dehydrogenase (R3)
	Other (see text)	Ribulose-5P kinase (R13)	2	–
			Total = 7	
Reductive TCA cycle				
	Carboxyl reduction + Carboxylation	Succinyl-CoA synthetase (B7)	1	2-Ketoglutarate synthase (A1)
		ATP citrate lyase (A4)	1	Pyruvate synthase (B1)
			Total = 2	
Dicarboxylate-4-hydroxypropionate cycle				
	Carboxylation	PEP synthetase (B2)	2	PEP carboxylase (B3)
	Carboxyl reduction	Succinyl-CoA synthetase (B7)	1	Succinyl-CoA reductase (C1)
	Carboxyl reduction + Carboxylation	Butyryl-CoA synthetase (C3)	1 (or 2†)	Pyruvate synthase (B1)
			total = 4 (5†)	
3-Hydroxypropionate-4-hydroxypropionate cycle*				
	Carboxylation	Acetyl-CoA carboxylase (D1)	2	Acetyl-CoA carboxylase (D1)
		Propionyl-CoA carboxylase (D7)	2	Propionyl-CoA carboxylase (D7)
	Carboxyl reduction	3-Hydroxypropionyl-CoA synthetase (D4)	1 (or 3†)	Succinyl-CoA reductase (C1)
		Butyryl-CoA synthetase (C3)	1 (or 2†)	Malonyl-CoA reductase (D2)
			Total = 6 (9†)	
3-Hydroxypropionate bicycle				
	Carboxylation	Acetyl-CoA carboxylase (D1)	2	Acetyl-CoA carboxylase (D1)
		Propionyl-CoA carboxylase (D7)	1	Propionyl-CoA carboxylase (D7)
	Carboxyl reduction	3-Hydroxypropionyl-CoA synthetase (D4)	2 (or 4†)	Malonyl-CoA reductase (D2)
			Total = 5 (7†)	
Reductive acetyl-CoA pathway of acetogens				
	Carboxyl reduction	Formate THF ligase (G2)	1	Methylenetetrahydrofolate Dehydrogenase (G4)
			Total = 1	
Reductive acetyl-CoA pathway of methanogens				
			Total = 0	
Glycine synthase pathway				
	Carboxyl reduction	Formate THF ligase (G2)	2	Methylenetetrahydrofolate Dehydrogenase (G4)
			total = 2	

The ATP hydrolyzing reactions in each pathway are classified according to the reaction type they energize (see main text). Enzymes that hydrolyze ATP molecules and enzymes that utilize the energy released by ATP hydrolysis to activate unfavorable reactions are shown. ‡Numbering in parentheses corresponds to enzyme numbering in Fig. 1. *The ATP cost of the 3-hydroxypropionate-4-hydroxypropionate cycle is calculated assuming that, in order to synthesize pyruvate, succinyl-CoA is diverted from the cycle and is oxidized to malate and oxaloacetate, which then undergoes decarboxylation to pyruvate [11,77]. †Assuming that pyrophosphate is hydrolyzed; hence, the hydrolysis of ATP to AMP and pyrophosphate correspond to the investment of two ATP equivalents.

reduction of succinate to succinate semialdehyde (Figs. 5 and 6B). In the 3-hydroxypropionate-4-hydroxybutyrate cycle the energy required to reduce succinate to succinate semialdehyde is invested through a different reaction: 3-hydroxypropionyl-CoA synthetase (enzyme 'D4' in Fig. 1B). Hence, the same unfavorable reaction may be coupled to different ATP hydrolysis reactions in different pathways (Fig. 5).

The converse is also true: different pathways may use the same ATP-hydrolyzing reaction to activate different downstream steps. For example, in the 3-hydroxypropionate bicycle, ATP hydrolysis by 3-hydroxypropionyl-CoA synthetase is not used to support the reduction of succinate to succinate semialdehyde, but rather the reduction of malonate to malonate semialdehyde many steps downstream (Figs. 4 and 5 and reaction 'D2' in Fig. 1B).

Unlike the acetyl-CoA–succinyl-CoA pathways that employ several different ATP-hydrolyzing reactions, the C1 carbon fixation pathways contain only one such reaction. Although not obvious at first glance, the ATP invested by formate-tetrahydrofolate ligase (reaction 'G2' in Fig. 1C) is used to energize the reduction of formate (carboxylic acid) to formaldehyde (carbonyl) (Fig. 4C). As compared to the bond between THF and formate (formyl-THF), the bond between THF and formaldehyde (methylene-THF) is energetically stable. Hence despite the difference in reduction potentials of the free metabolites, the reduction of formyl-THF to methylene-THF using NAD(P)H as an electron donor (reactions 'G3' and 'G4' in Fig. 1C) is almost energy neutral ($\Delta_r G'^m \sim 0$, Fig. 6C). As the bond between THF and formate is relatively unstable, its formation has to be energized by its coupling to ATP hydrolysis (Fig. 6C). Hence, like the thioester bond, the energy released by ATP hydrolysis is temporarily stored in the bond between formate and THF and is later used to reduce the molecule to methylene-THF (Fig. 6C).

The reductive pentose phosphate pathway contains two unique ATP hydrolyzing reactions. The first, catalyzed by glycerate 3-phosphate kinase (reaction 'R2' in Fig. 1A), transfers a phosphate group from ATP to activate glycerate 3-phosphate, forming an anhydride bond. In the next step (reaction 'R3' in Fig. 1A), this bond is hydrolyzed, providing the energy required for the reduction of the carboxyl to an aldehyde (Fig. 6D). Notably, the reductive pentose phosphate pathway is the only known carbon fixation pathway that hydrolyzes ATP for purposes other than carboxylation or carboxyl reduction. The phosphorylation of ribulose 5-phosphate to ribulose 1,5-bisphosphate (reaction 'R13' in Fig. 1A) does not energize a carboxylation or a carboxyl reduction.

3.4. Bypassing ATP hydrolysis by coupling unfavorable carboxylation and carboxyl reduction to other exergonic reactions

The net reaction for pyruvate formation, $3\ CO_2 + 5\ A^{red} \rightarrow$ Pyruvate $+ 3\ H_2O + 5\ A^{ox}$, 'A' being NADP or a pair of ferredoxins, has a $\Delta_r G'^m \leq 80$ kJ/mol (pH 7), and requires an investment of at most two ATP molecules to achieve thermodynamic feasibility (the hydrolysis

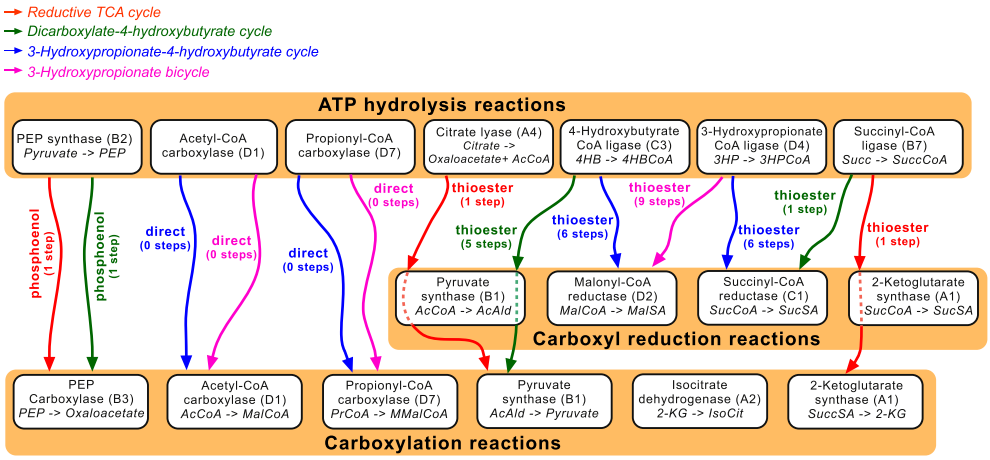

Fig. 5. Linkage between ATP hydrolyzing reactions and the carboxylations and carboxyl reductions they energize in the acetyl-CoA–succinyl-CoA pathways. Enzyme names, enzyme numbering according to Fig. 1B and the biochemical transformation they catalyze are given in boxes. Arrows correspond to the 'flow of energy' from ATP hydrolysis reaction to the reaction it energizes. The color of the arrow represents the pathway in which the energetic linkage exists. Labels near the arrow describe the bond that temporarily stores the energy, while the number in parentheses represents the number of reaction steps separating the ATP hydrolysis reaction to the reaction it energizes. Some ATP hydrolyzing reactions energize consecutive carboxyl reduction and carboxylation (see main text). These cases are indicated by a solid–dashed–solid line. The carboxylation of 2-ketoglutarate by isocitrate dehydrogenase is not coupled to ATP hydrolysis but rather to another exergonic reaction (see main text). Notably, in different pathways the same unfavorable reaction might be supported by ATP hydrolysis in different reactions. Also, in different pathways the same ATP hydrolysis reaction can support different unfavorable reactions. Abbreviations: AcCoA: acetyl-CoA; 4HB: 4-hydroxybutyrate; 4HBCoA: 4-hydroxybutyryl-CoA; 3HP: 3-hydroxypropionate; 3HPCoA: 3-hydroxypropionyl-CoA; Succ: succinate; SuccCoA: succinyl-CoA; AcAld: acetaldehyde; MalCoA: malonyl-CoA; MalSA: malonate semialdehyde; SucSA: succinate semialdehyde; PrCoA: propionyl-CoA; MMalCoA: methylmalonyl-CoA; 2-KG: 2-ketoglutarate; IsoCit: isocitrate.

of an ATP releases ~50 kJ/mol) [12]. However, according to the above analysis, the ATP consumption of a carbon fixation pathway is not only affected by the net reaction, but rather is related to the number of carboxylations and carboxyl reductions in the pathway. Hence, one might expect the total ATP consumption of a pathway to match the number of these reactions used. As discussed above, non-C1 pathways generally require three carboxylations and two carboxyl reductions for the production of pyruvate, suggesting that five ATP molecules should to be hydrolyzed to achieve thermodynamic feasibility.

Yet, while many carbon fixation pathways contain this exact number of carboxylation and carboxyl reduction steps, some pathways invest more or less ATP than others. Occasionally, more than one ATP molecule is consumed to activate an unfavorable reaction. For example, two ATP equivalents are invested in the carboxylation of pyruvate to oxaloacetate, the energy of which is temporarily stored in the phosphoenol group of PEP (reactions 'B2' and 'B3' in Fig. 1B).

On the other hand, some pathways exhibit lower-than-expected ATP requirements. This can be achieved if one or more unfavorable reaction steps are coupled to exergonic reactions other than ATP hydrolysis [10]. For example, the enzyme isocitrate dehydrogenase (reaction 'A2' in Fig. 1B) mechanistically couples two sequential reactions: the carboxylation of 2-ketoglutarate to oxalosuccinate and the reduction of oxalosuccinate to isocitrate (Figs. 4B and 6E). Although the carboxylation step is extremely unfavorable ($\Delta_rG'^m = +63$ kJ/mol) the reduction to which it is coupled (carbonyl reduction to hydroxycarbon using NADPH) releases enough energy to compensate for most of the energy gap ($\Delta_rG'^m = -42$ kJ/mol, Fig. 6E). While the overall reaction catalyzed by isocitrate dehydrogenase is endergonic under 1 mM reactant concentrations ($\Delta_rG'^m = +21$ kJ/mol) this energetic barrier is low enough that it can be overcome by altering reactant concentrations within the physiological range (Methods).

The enzymes pyruvate synthase and 2-ketoglutarate synthase (enzymes 'B1' and 'A1' in Fig. 1B, respectively) provide two more interesting examples of bypassing a carboxylation-related ATP investment. These enzymes couple carboxylation to the activated reduction of a carboxyl, as shown in Fig. 6F [10]. Therefore, the hydrolysis of the thioester bond energizes both the unfavorable reduction and the unfavorable carboxylation (Fig. 4B). Importantly, the energy released by thioester hydrolysis is lower than the energy required for the consecutive carboxyl reduction and carboxylation (net $\Delta_rG'^m = +14$ kJ/mol). However, as in the case of isocitrate dehydrogenase, this energy barrier is surmountable within the physiological concentration range of metabolites.

The reductive pentose phosphate pathway does not invest even a single ATP in carboxylation. The carboxylating enzyme Rubisco (reaction 'R1' in Fig. 1A) couples the unfavorable carboxylation reaction (transforming Ribulose 1,5-bisphosphate to 2-carboxy-3-ketoarabinitol 1,5-bisphosphate, $\Delta_rG'^m \sim +30$ kJ/mol, Fig. 6G) with the very favorable cleavage of a carbon–carbon bond in which a carbonyl is oxidized to a carboxyl (transforming 2-carboxy-3-ketoarabinitol 1,5-bisphosphate to two molecules of glycerate 3-phosphate, $\Delta_rG'^m \sim -70$ kJ/mol, Fig. 6G) [51]. Yet, there is no net ATP savings in this approach. This is because the carboxyl formed by Rubisco must be re-reduced to a carbonyl later in the pathway, requiring extra ATP-consuming reactions. Indeed, five carboxyl reductions (reaction 'R3' in Fig. 1A) are required to produce one pyruvate molecule through the reductive pentose phosphate pathway instead of the expected two. In a sense, the carbonyl carries the energy released by ATP hydrolysis (like a thioester bond), such that its oxidation energizes the carboxylation catalyzed by Rubisco.

In some cases the ATP investment needed for carboxyl reduction can also be deferred. For example, the cleavage of acetoacetyl-CoA (reaction 'C7' in Fig. 1B) involves the oxidation of a carbonyl to a carboxyl which releases a significant amount of energy ($\Delta_rG'^m = -78$ kJ/mol, Fig. 4). This energy can be used to establish a thioester bond. Therefore, the cleavage of acetoacetyl-CoA results in the formation of two acetyl-CoA molecules instead of one acetyl-CoA and one acetate. In the dicarboxylate-4-hydroxybutyrate cycle, for example, this thioester energizes the carboxyl reduction and carboxylation catalyzed by pyruvate synthase, thereby bypassing ATP hydrolysis. However, as in the case of Rubisco, there is no net ATP savings in this approach: an extra ATP-dependent carboxyl reduction is required to balance the carbonyl oxidation in acetoacetyl-CoA cleavage.

3.5. The C1 carbon fixation pathways bypass most ATP-hydrolysis reactions

The C1 carbon fixation pathways employ multiple mechanisms to bypass ATP-dependent reactions, resulting in a very low ATP requirement (Table 1). First, directly reducing CO_2 to formate (reaction 'G1' in Fig. 1C) bypasses an ATP-requiring carboxylation reaction. As discussed above, the reduction of CO_2 to formate does not follow the general trend of a decreasing reduction potential with increasing oxidation

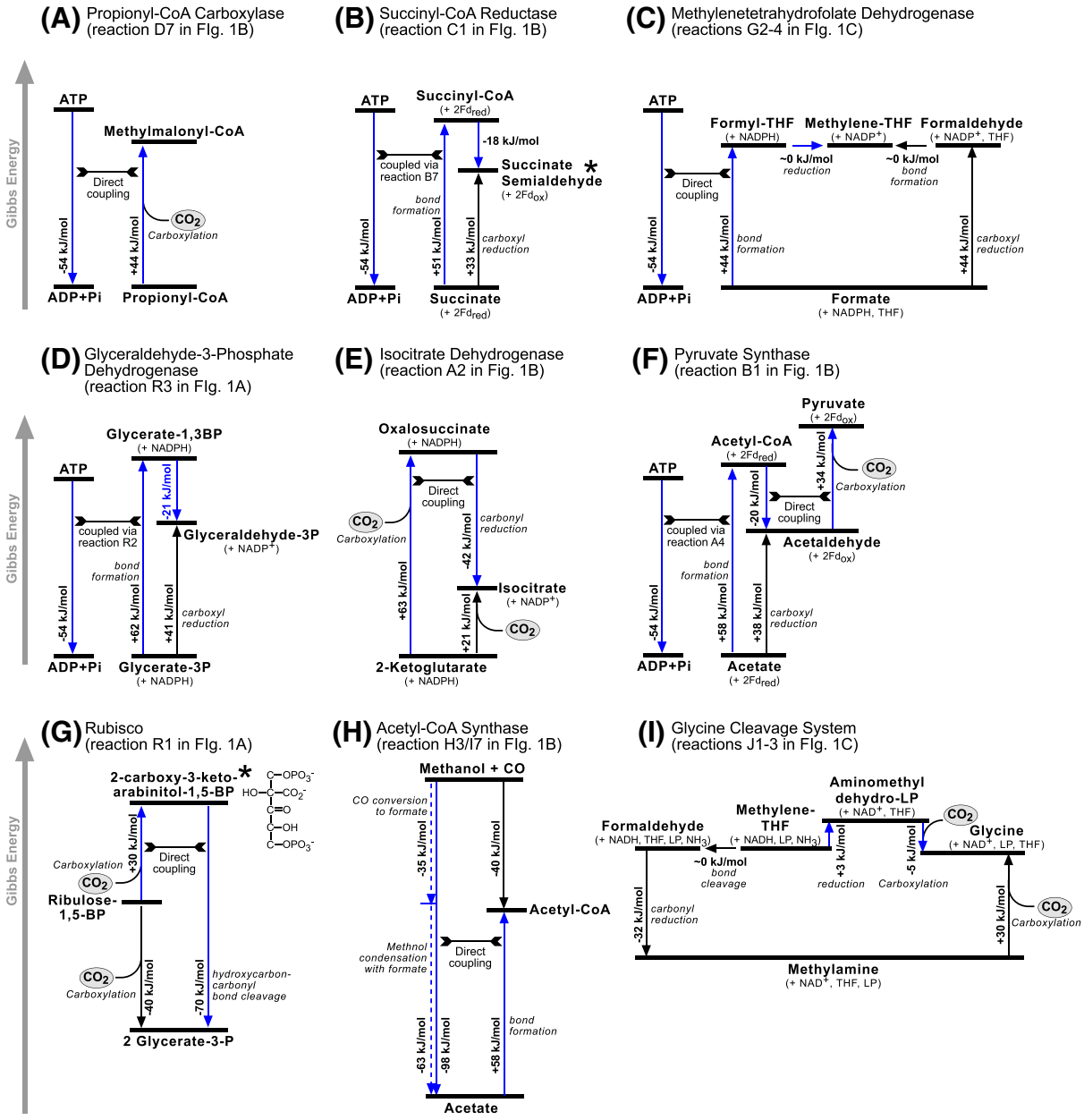

Fig. 6. Mechanisms for activating unfavorable reactions through coupling to energy releasing transformations. Changes in Gibbs energy under reactant concentrations of 1 mM, $\Delta_rG'^m$, are shown [34]. Blue arrows represent the biochemical transformations which take place *in vivo*. Reaction types are written near the arrows. Δ_fG' values for compounds marked with '*' were calculated using group contribution [39]. All other Δ_fG' values were experimentally derived. $\Delta_rG'^m$ values for the THF system ('C' and 'I') were taken from [41] while $\Delta_rG'^m$ values for the glycine cleavage system ('I') were taken from [40].

state. In fact, the reduction of CO_2 to formate is much more favorable than carboxylation or carboxyl reduction (Figs. 2 and 3). The moderate $\Delta_rG'^m$ barrier associated with the reduction of CO_2 to formate using NADPH ($\Delta_rG'^m$<20 kJ/mol) can be overcome by operating at high [CO_2] and keeping [formate] low. Indeed, none of the C1 pathways activate the reduction of CO_2 to formate with ATP hydrolysis, thereby saving an ATP that would otherwise be invested in carboxylation. In these pathways, CO_2 is reduced twice or three times with an investment of a single ATP (required for the reduction of formate, see above), and the resulting C1 moiety is then ligated with an acceptor molecule in a favorable reaction.

On the other hand, the reduction of CO_2 to CO with ferredoxin (reaction 'H2'/'I6' in Fig. 1C) is as thermodynamically challenging as carboxyl reduction ($\Delta_rG'^m \sim +38$ kJ/mol, Fig. 2). Yet, no ATP is hydrolyzed to energize this reduction. By keeping CO as a bound intermediate (bound to the prosthetic group corrinoid) the CO-dehydrogenase–acetyl–CoA-synthase complex couples this reduction to the highly exergonic acetyl-CoA synthase reaction ($\Delta_rG'^m < -50$ kJ/mol, reaction 'H3'/'I7' in Fig. 1C). (The bound CO intermediate most likely has lower Gibbs energy as compared to free CO, enabling a decrease in the $\Delta_rG'^m$ of CO_2 reduction at the expense of an increase in the $\Delta_rG'^m$ for acetyl-CoA synthase.) The resulting net reaction is favorable in the direction of fixation.

The reductive acetyl-CoA pathway saves yet another ATP by coupling the formation of the thioester of acetyl-CoA to the formation of acetate from 5-Methyl-THF and CO (reaction 'H3'/'I7' in Fig. 1C). 5-Methyl-THF is a methanol ligated with the C1 carrier THF. If we neglect the energetic effect of the carrier (5-Methyl-THF cleavage to THF and methanol seems to be close to energy neutral), we find that the condensation of methanol and CO is extremely exergonic, $\Delta_rG'^m \sim -100$ kJ/mol (Fig. 6H). The energy released in this reaction can be attributed to two factors. First, the transformation of CO into a formate releases a considerable amount of energy ($\Delta_rG'^m \sim -35$ kJ/mol, Fig. 6H) as expected by

the differences in the reduction potentials (Fig. 2). Second, in contrast to unfavorable carboxylation reactions in which CO_2 is reduced and ligated with another carbon, the reduction and ligation of methanol to another carbon is highly favorable (-65 kJ/mol$<\Delta_rG'^m<-30$ kJ/mol, Fig. 3). The energy released by the overall reaction is sufficient to energize both the formation of a thioester (acetyl-CoA) and the unfavorable reduction of CO_2 to CO (see above).

Altogether, the reductive acetyl-CoA pathway represents the most extreme example of a reduced ATP investment. Acetogens operating the pathway invest only a single ATP molecule during the formation of pyruvate (when attaching formate to THF). Methanogens operating the pathway bypass ATP investment altogether, directly reducing CO_2 and attaching it to a C1 carrier (Fig. 1C). Even though this reaction is energized by using the low reduction potential ferredoxin as an electron donor, it is extremely unfavorable ($\Delta_rG'^m\sim+45$ kJ/mol) and can only take place via coupling to other exergonic reactions [52].

The glycine synthase pathway invests two ATP molecules in the formation of pyruvate; both are consumed in the attachment of formate to THF (Fig. 1C). The only carboxylation reaction involved in the glycine synthase pathway (reaction 'J2' in Fig. 1C) does not require ATP investment since it is coupled to another exergonic reaction. The substrate of this carboxylation is methylamine attached to a lipoic acid, which is carried by the H-protein of the glycine cleavage system [53]. The carboxylation of free methylamine (to form glycine) is unfavorable and requires activation ($\Delta_rG'^m\sim+30$ kJ/mol, Fig. 6I). However, the reaction preceding carboxylation is the reduction of a carbonyl (formaldehyde ligated with THF) to an aminocarbon (reaction 'J1' in Fig. 1C). Since the reduction potential of a carbonyl to an aminocarbon is similar to that of a carbonyl to a hydroxycarbon (under ammonia concentration of 1 mM the conversion of a hydroxycarbon to an aminocarbon is close to energy neutral), energy is released by reducing a carbonyl to an aminocarbon using NAD(P)H ($\Delta_rG'^m\sim-32$ kJ/mol, Fig. 6I). This energy is stored in the bond between the methylamine moiety and the lipoic acid and is used to activate the carboxylation reaction without ATP investment (Fig. 6I).

4. Discussion

The net carbon fixation reaction does not require much ATP investment to become favorable; the formation of pyruvate from CO_2 requires 0–2 ATPs depending on the cellular and environmental conditions. However, in this study we demonstrated that overall pathway thermodynamics, from substrate(s) to final product(s), cannot explain the ATP requirement of most carbon fixation pathways. Instead, analogous to the overpotential required in electron transfer reactions, extra ATP investment is needed to overcome the energy barriers of the specific reactions that constitute the pathway. Specifically, carbon fixation pathways contain two types of energetically challenging reactions: carboxylation and carboxyl reduction. Generally five such unfavorable reactions are required to reduce CO_2 to pyruvate, suggesting that carbon fixation should invest at least five ATPs per pyruvate. This explains why some pathways invest considerably more ATP than expected given their net reactions: the ATP consumption of these pathways is governed by the local thermodynamic barriers they contain. Yet, other pathways expend less than five ATPs to fix carbon. This is only possible because they sidestep thermodynamically challenging reactions by coupling them to exergonic reactions other than ATP-hydrolysis (*e.g.* isocitrate dehydrogenase) or by using alternative metabolic routes (*e.g.* CO_2 reduction to formate instead of a carboxylation reaction). Nonetheless, these pathways are still limited by the thermodynamics of the net carbon fixation reaction: the ATP consumption of these pathways is governed by their overall net reaction rather than local barriers.

With the exception of the reductive pentose phosphate cycle, all the ATP molecules hydrolyzed by all carbon fixation pathways are directly or indirectly coupled to carboxylation or carboxyl reduction. Yet, the mechanisms for this coupling are numerous and vary from one pathway to the next. Acetyl-CoA and propionyl-CoA carboxylases, for example, directly couple ATP hydrolysis to carboxylation. Yet, in most pathways the coupling is achieved indirectly: ATP hydrolysis establishes a bond with high energy-of-hydrolysis which is later hydrolyzed by the enzyme catalyzing the unfavorable reaction. These energy-carrying bonds include thioesters (reactions 'B7', 'C3' and 'D4' in Fig. 1), phosphoenols (reaction 'B1'), phosphoanhydrides (reaction 'R2'), the bond between formate and THF (reaction 'G2') and the bond between methylamine and lipoic acid (reaction 'I1').

A close inspection reveals that the activation of all carboxyl reduction reactions involved in carbon fixation is done by indirect coupling to ATP hydrolysis. Given that enzymes that directly couple carboxyl reduction to ATP hydrolysis do exist [54–56], it is puzzling why indirect coupling is so prevalent. Since the mechanism for such a direct coupling is rather complicated [54–56], it is possible that indirect coupling is more common because it is mechanistically simpler. Indirect coupling might also provide secondary benefits. Both CoA and phosphate were found to significantly increase the affinity of the enzymes towards the substituted substrates [57]. Hence, indirect coupling through CoA-substituted or phosphorylated metabolites might offer the advantage of improved kinetics. Future studies may shed light on the logic behind the abundance of indirect coupling.

We found many examples in which ATP investment is bypassed by a direct coupling of unfavorable reactions to exergonic reactions other than ATP hydrolysis. If the endergonic and exergonic reactions take place sequentially they can be directly coupled by an enzyme carrying out both reactions in the same active site without releasing the intermediate. This sort of coupling appears often when an unfavorable carboxylation reaction is energized by a favorable oxidoreductase reaction which follows it [10]. The oxidoreductase reaction can involve a carbonyl reduction, a hydroxycarbon reduction, a CoA-activated carboxyl reduction or a carbonyl oxidation to a non-activated carboxyl. Isocitrate dehydrogenase, homoisocitrate dehydrogenase, malic enzyme, 3-isopropylmalate dehydrogenase, 3-methylmalate dehydrogenase, 2,3-dimethylmalate dehydrogenase and phosphogluconate dehydrogenase serve as examples in which the energy released by carbonyl reduction (using NAD(P)H) energizes carboxylation such that the overall reaction is reversible ($+15$ kJ/mol$<\Delta_rG'^m<+20$ kJ/mol). Indeed, isocitrate dehydrogenase and malic enzyme are known to carry flux in the reductive direction *in-vivo* in various organisms and under specific conditions [58–62]. A similar coupling was recently demonstrated to be part of the crotonyl-CoA carboxylase/reductase mechanism. This enzyme couples an unfavorable carboxylation with an energy releasing NAD(P)H-dependent reduction of a double bond to a hydrocarbon (equivalent to the reduction of a hydroxycarbon to a hydrocarbon since the dehydration of an hydroxycarbon into an alkene is mostly an energy neutral process, $|\Delta_rG'^m|<10$ kJ/mol), making the overall process favorable ($\Delta_rG'^m\sim-20$ kJ/mol) [63,64].

The reduction potential of CoA-activated carboxyls (-350 mV$<E'^m<-250$ mV) is considerably higher than that of un-activated carboxyls since the hydrolysis of the thioester bond energizes the reduction. In fact, the reduction potential of CoA-activated carboxyls is higher than that of ferredoxin and similar to that of NAD(P)H. Therefore, using ferredoxin (but not NAD(P)H) to reduce a CoA-activated carboxyl is sufficient to energize carboxylation. Pyruvate and 2-ketoglutarate synthases (discussed above) exemplify this approach, where the hydrolysis of the thioester energizes both carboxyl reduction and carboxylation. Conversely, the energy released by the oxidation of a carbonyl to a non-activated carboxyl can also energize a carboxylation reaction. Perhaps the best example for this coupling is catalyzed by Rubisco: the cleavage of a carbon–carbon bond in which the oxidation of a carbonyl to a carboxyl is directly coupled to carboxylation, making the overall reaction highly favorable.

The coupling between an unfavorable reaction and an exergonic reaction other than ATP hydrolysis can also be indirect: two consecutive reactions that take place at different active sites but within the

same protein complex can be coupled via substrate channeling. Substrate channeling enables the effective concentration of an intermediate to breach the normal physiological limit on metabolite concentrations, allowing it to attain a wider range of energy levels. A good example of substrate channeling is the CO-dehydrogenase–acetyl-CoA-synthase complex, discussed above, which couples the unfavorable CO_2 reduction to CO with the highly exergonic acetyl-CoA synthesis. Many enzymes of the reductive pentose phosphate pathway also operate in complexes and channel substrates between different active sites [65]. Future studies might elucidate how exactly substrate channeling affects the energetics of pathways and how common the phenomenon is in carbon fixation pathways.

Overall, we discussed several mechanisms that can be used to activate an unfavorable reaction. Table 2 summarizes them. Notably, carbon fixation pathways make use of all of these mechanisms, illustrating the diversity of energetic approaches to this central biological process.

We stress that our analysis did not consider distributed thermodynamic bottlenecks: an energetic barrier composed of several reactions [8]. For example, the consecutive operation of 2-ketoglutarate synthase (reaction 'A1' in Fig. 1B) and isocitrate dehydrogenase (reaction 'A2'), as in the reductive TCA cycle, represent a cumulative $\Delta_rG'^m$ of over 40 kJ/mol. One approach that enables these reactions to proceed simultaneously without further activation is to keep the cellular pH well below 7. As shown in Fig. 7, CO_2 and carboxyl reduction are much more favorable at pH 6 than at pH 7. At pH 6, for example, the consecutive operation of 2-ketoglutarate synthase and isocitrate dehydrogenase has $\Delta_rG'^m \sim 28$ kJ/mol, within the reversible range. It is therefore likely that many of the organisms which operate the TCA cycle operate at cytosolic pH lower than 7.

Throughout this study we referred to ATP hydrolysis as a well-defined reaction in which ATP is hydrolyzed to ADP and Pi. However, some enzymes hydrolyze ATP to AMP and pyrophosphate. This alternative alters the energetic profile of the reaction and might result in a higher ATP cost for the overall pathway [11–13]. Specifically, the acetyl-CoA–succinyl-CoA pathways utilize two enzymes that hydrolyze ATP to AMP and pyrophosphate (reactions 'C3' and 'D4' in Fig. 1B). The cellular fate of pyrophosphate in organisms that employ these pathways is still unclear [13]. Pyrophosphate (PPi) can either be used as an energy source, like ATP [66–71], or it can be directly hydrolyzed by a pyrophosphatase enzyme to inorganic phosphate, dissipating its energy. The latter option effectively increases the energy released by ATP hydrolysis as the reaction ATP => AMP + 2 Pi has an associated $\Delta_rG'^m \sim -105$ kJ/mol. However, this approach also increases the ATP cost of the pathway: two ATP equivalents are invested instead of one. It seems unlikely that the extra energetic push of pyrophosphate hydrolysis is required for the acetyl-CoA–succinyl-CoA pathways and hence it is tempting to suggest that pyrophosphate is not hydrolyzed, considerably decreasing the ATP requirement of the pathways (Table 1).

If pyrophosphate is indeed not hydrolyzed immediately by organisms utilizing the acetyl-CoA–succinyl-CoA pathways, the reductive pentose phosphate pathway is the most ATP-costly of all carbon fixation pathways, hydrolyzing 7 ATPs in the synthesis of pyruvate (Table 1). This high ATP requirement is not surprising since the reductive pentose phosphate pathway is also the only carbon fixation pathway that invests ATP in metabolic aims other than carboxylation or carboxyl reduction. The ATP molecules hydrolyzed by phosphoribulokinase (reaction 'R13' in Fig. 1A) serve to keep all the pathway metabolites phosphorylated and to establish irreversible reactions along the pathway. These apparently "non-essential" ATP hydrolysis steps make the reductive pentose phosphate pathway appear the least ATP efficient of all the carbon fixation pathways. However, a closer look suggests that these steps may be essential.

While charged compounds cannot pass through the hydrophobic lipid membrane and are hence trapped within the cell, uncharged molecules, like sugars, can escape the cell much more easily [72–74]. The acetyl-CoA–succinyl-CoA pathways and the C1 carbon fixation pathways do not contain even a single uncharged free metabolite. On the other hand, without the extra phosphorylation step of phosphoribulokinase all the sugar intermediates of the reductive pentose phosphate pathway would be unphosphorylated and, as such, uncharged. Therefore, the extra ATP molecules invested by the reductive pentose phosphate pathway can be regarded as a solution to a problem other carbon fixation pathways may not encounter, *i.e.* metabolite leakage [75,76].

Table 2
Mechanisms of activating unfavorable reactions.

Increasing substrate concentrations and decreasing product concentrations	
Applicability	Example
When the reaction is only moderately unfavorable, $\Delta_rG'^m < +30$ kJ/mol, so that required metabolite concentrations are not too low or high	Oxidation of malate to oxaloacetate using NAD^+ as an electron acceptor
Direct coupling to ATP hydrolysis	
Applicability	Example
When an enzymatic mechanism for such a coupling is available	Acetyl-CoA carboxylase
Indirect coupling to ATP hydrolysis: ATP hydrolysis is coupled to the formation of a bond with high energy of hydrolysis, whose hydrolysis is coupled to the unfavorable reaction	
Applicability	Example
When the metabolite contains a functional group that can establish a bond with high energy of hydrolysis (the formation of a thioester, for example, requires a carboxyl group)	Succinyl-CoA synthetase catalyzes the ATP-dependent formation of a thioester bond between succinate and CoA, which is later hydrolyzed by succinyl-CoA reductase
Direct coupling to an exergonic reaction other then ATP hydrolysis	
Applicability	Example
When the exergonic reaction directly precedes or follows the unfavorable reaction in the pathway and when an enzymatic mechanism for such a coupling is available	Isocitrate dehydrogenase couples carboxylation with carbonyl reduction
Indirect coupling to an exergonic reaction other then ATP hydrolysis: substrate channeling within a protein complex	
Applicability	Example
When the exergonic reaction(s) directly precedes or follows the unfavorable reaction(s) in the pathway	CO-dehydrogenase–acetly-CoA-synthase complex couples the unfavorable CO_2 reduction to CO with the highly exergonic acetyl-CoA synthesis

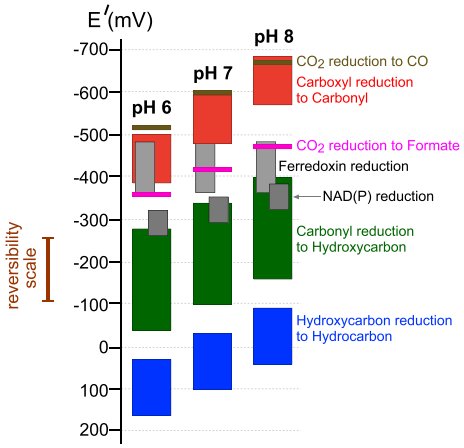

Fig. 7. The reduction potentials, E'^0, of electron carriers and half-reactions at varying pH. See Fig. 2 for details. The pH dependence of the reduction potential of each functional group and electron carrier is described in the Methods.

5. Conclusions

The analysis presented here demonstrates that the energetic requirements of a pathway can be assessed by analyzing the reaction types it employs in order to achieve its metabolic aims. Examining the generalized reaction types contained in a pathway enables fast estimation of the number of ATP molecules that are expected to be invested. By examining natural pathways in this manner, we further uncovered several mechanisms that pathways employ to reduce their ATP requirement. We demonstrated this approach by applying it to natural carbon fixation pathways. Such an approach can also be applied to the analysis of other types of metabolic pathways. For example, instead of considering reductive processes like carbon fixation, one can apply the same principles to investigate the energetic constraints imposed on oxidative metabolism. In addition, our methodology is especially useful in metabolic engineering efforts as it enables fast assessment of the energetic resources required by synthetic pathways and offers several mechanisms for bypassing energetically challenging reactions through coupling to exergonic reactions other than ATP hydrolysis.

Acknowledgements

We thank Dan Tawfik and Tobias Erb for helpful discussions and critique regarding the manuscript. A.B.-E. is supported by the Adams Fellowship Program of the Israel Academy of Sciences and Humanities. E.N. is grateful to the Azrieli Foundation for the award of an Azrieli Fellowship. This study was supported by the European Research Council (Grant 260392-SYMPAC), and by the Israel Science Foundation (Grant 750/09). R.M is the incumbent of the Anna and Maurice Boukstein career development chair.

Appendix 1. Experimentally derived reduction potentials and $\Delta_r G'^m$ for carbon–carbon formation reactions

Values calculated from experimentally derived Gibbs energies of formation [36] and from experimentally derived equilibrium constants [35].

	Reduction potential in mV
CO2 reduction	
$CO_2 + 2e^- <=> CO + H_2O$	−596
$CO_2 + 2e^- <=>$ formic acid	−415
Carboxyl reduction to carbonyl	
Acetate + $2e^- <=>$ acetaldehyde + H_2O	−598
Butyrate + $2e^- <=>$ butanal + H_2O	−559
Glycerate + $2e^- <=>$ D-glyceraldehyde + H_2O	−550
Formate + $2e^- <=>$ formaldehyde + H_2O	−547
Glycerate 3-phosphate + $2e^- <=>$ glyceraldehyde 3-phosphate + H_2O	−533
6-Phospho-D-gluconate + $2e^- <=>$ D-glucose 6-phosphate + H_2O	−497
Oxalate + $2e^- <=>$ glyoxylate + H_2O	−475
Carbonyl reduction to hydroxycarbon	
Succinate semialdehyde + $2e^- <=>$ 4-hydroxybutanoic acid	−334
(13E)-11alpha-hydroxy-9,15-dioxoprost-13-enoate + $2e^- <=>$ alprostadil	−325
Androstenedione + $2e^- <=>$ testosterone	−309
Estrone + $2e^- <=>$ estradiol-17beta	−309
3-Hydroxybenzaldehyde + $2e^- <=>$ 3-hydroxybenzyl alcohol	−301
5-Dehydroshikimate + $2e^- <=>$ shikimate	−289
Acetone + $2e^- <=>$ isopropanol	−288
Cyclohexanone + $2e^- <=>$ cyclohexanol	−286
D-Fructose + $2e^- <=>$ mannitol	−280
D-Fructose 6-phosphate + $2e^- <=>$ D-mannitol 1-phosphate	−278
Retinal + $2e^- <=>$ retinol	−276
D-Fructose + $2e^- <=>$ mannitol	−275
D-Tagatose + $2e^- <=>$ galactitol	−275
D-Glucose 6-phosphate + $2e^- <=>$ D-sorbitol 6-phosphate	−269
Acetoacetate + $2e^- <=>$ (R)-3-hydroxybutanoate	−268
L-Sorbose + $2e^- <=>$ L-iditol	−267
D-Glucose + $2e^- <=>$ D-sorbitol	−262
D-Fructose + $2e^- <=>$ D-sorbitol	−260
Sepiapterin + $2e^- <=>$ 7,8-dihydrobiopterin	−259
Coniferyl aldehyde + $2e^- <=>$ coniferyl alcohol	−257
2-keto-D-Gluconic acid + $2e^- <=>$ D-gluconic acid	−253
D-Fructose 6-phosphate + $2e^- <=>$ D-sorbitol 6-phosphate	−253
3-Dehydroquinate + $2e^- <=>$ quinate	−249
(R)-Acetoin + $2e^- <=>$ (R,R)-butane-2,3-diol	−241
D-Xylose + $2e^- <=>$ xylitol	−238
D-Ribulose + $2e^- <=>$ D-arabitol	−239
Acetoacetyl-CoA + $2e^- <=>$ (S)-3-hydroxybutanoyl-CoA	−236
L-Xylulose + $2e^- <=>$ xylitol	−234
5-Dehydro-D-Fructose + $2e^- <=>$ D-Fructose	−233
2-Dehydropantoate + $2e^- <=>$ (R)-pantoate	−232
L-Aspartate 4-semialdehyde + $2e^- <=>$ L-homoserine	−216
D-Ribulose + $2e^- <=>$ ribitol	−226
Benzaldehyde + $2e^- <=>$ benzyl alcohol	−225
2-Oxobutanoate + $2e^- <=>$ 2-hydroxybutanoic acid	−224
2-Methyl-3-oxopropanoate + $2e^- <=>$ 3-hydroxy-2-methylpropanoate	−222
3-Oxohexanoyl-CoA + $2e^- <=>$ (S)-hydroxyhexanoyl-CoA	−221
3-Dehydro-L-threonate + $2e^- <=>$ threonate	−221
3-Dehydrocarnitine + $2e^- <=>$ L-carnitine	−205
1-Octanal + $2e^- <=>$ 1-octanol	−205
Butanal + $2e^- <=>$ 1-butanol	−203
3-Hexenal + $2e^- <=>$ 3-hexenol	−199
Acetaldehyde + $2e^- <=>$ ethanol	−199
3-Oxopropanoate + $2e^- <=>$ 3-hydroxypropanoate	−199
Glycerone phosphate + $2e^- <=>$ sn-glycerol 3-phosphate	−195
3-Dehydrocarnitine + $2e^- <=>$ (S)-carnitine	−192
Pyruvate + $2e^- <=>$ R-lactate	−190
Formaldehyde + $2e^- <=>$ methanol	−188
Pyruvate + $2e^- <=>$ (S)-lactate	−187
3-dehydro-2-deoxy-D-gluconate + $2e^- <=>$ 2-deoxy-D-gluconate	−187
Dihydroxyacetone + $2e^- <=>$ glycerol	−179
(S)-Lactaldehyde + $2e^- <=>$ propane-1,2-diol	−179
2-Oxoglutarate + $2e^- <=>$ (S)-2-hydroxyglutarate	−178
Pyridoxal + $2e^- <=>$ pyridoxine	−174
2,5-didehydro-D-gluconate + $2e^- <=>$ 2-dehydro-L-idonate	−169
Oxaloacetate + $2e^- <=>$ malate	−164
2-hydroxy-3-oxopropanoate + $2e^- <=>$ D-glycerate	−156
3,5-diiodo-4-hydroxyphenylpyruvate + $2e^- <=>$ 3-(3,5-diiodo-4-hydroxyphenyl)lactate	−155
Hydroxypyruvate + $2e^-$ = glycerate	−148
3-Phosphonooxypyruvate + $2e^- <=>$ 3-phospho-D-Glycerate	−145
D-Glyceraldehyde + $2e^- <=>$ Glycerol	−123
2-hydroxy-3-Oxosuccinate + $2e^- <=>$ meso-Tartaric acid	−119
Oxalosuccinate + $2e^- <=>$ Isocitrate	−105
Glyoxylate + $2e^- <=>$ Glycolate	−97
Hydroxycarbon reduction to hydrocarbon	
Glycolate + $2e^- <=>$ Acetate + H2O	−29
½ Glycerol + $2e^- <=>$ ½1-Propanol + H_2O	−25
½ Glycerol + $2e^- <=>$ ½ Isopropanol + H_2O	0
Malyl-CoA + $2e^- <=>$ Succinyl-CoA + H_2O	12
Malate + $2e^- <=>$ Succinate + H_2O	20
½ Dihydroxyacetone + $2e^- <=>$ ½ Acetone + H_2O	54
Glycerate + $2e^- <=>$ L-Lactate + H_2O	61
Glycerate + $2e^- <=>$ 3-Hydroxypropanoate + H_2O	70
Methanol + $2e^- <=>$ Methane + H_2O	78

(continued on next page)

Appendix 1 (*continued*)

	$\Delta_r G'^m$ in kJ/mol
L-Serine + $2e^-$ <=> L-Alanine + H_2O	84
Hydroxypyruvate + $2e^-$ <=> Pyruvate + H_2O	103
Carboxylations (co_2 reudction and condensation)	
CO2(total) + Formaldehyde <=> Glyoxylate + H_2O	29
CO2(total) + Methylamine <=> Glycine + H_2O	30
CO2(total) + Ethanol <=> 3-Hydroxypropanoate + H_2O	30
CO2(total) + Methane <=> Acetate + H_2O	32
CO2(total) + Ethanol <=> l-Lactate + H_2O	32
CO2(total) + Acetaldehyde <=> Pyruvate + H_2O	34
CO2(total) + 3-Hydroxypropanoate <=> Malate + H_2O	42
CO2(total) + Formate <=> Oxalate + H_2O	43
CO2(total) + l-Lactate <=> Malate + H_2O	40
CO2(total) + Propanoyl-CoA <=> Methylmalonyl-CoA + H_2O	44
CO2(total) + Pyruvate <=> Oxaloacetate + H_2O	45
CO2(total) + 2-Oxoglutarate <=> Oxalosuccinate + H_2O	63
Carboxyl reduction and condensation	
2 Formate <=> Glyoxylate + H_2O	55
Oxalate + Methane <=> Pyruvate + H_2O	58
Oxalate + Methanol <=> Hydroxypyruvate + H_2O	63
Acetate + Methane <=> Acetone + H_2O	65
Formate + Methane <=> Acetaldehyde + H_2O	67
Formate + Acetate <=> Pyruvate + H_2O	69
Oxalate + Acetate <=> Oxaloacetate + H_2O	71
Glycolate + Methanol <=> Dihydroxyacetone + H_2O	76
2 Acetate <=> Acetoacetate + H_2O	78
Acetate + Acetyl-CoA <=> Acetoacetyl-CoA + H_2O	85
Formate + Glycolate <=> Hydroxypyruvate + H_2O	95
Carbonyl reduction and condensation	
Formaldehyde + D-Xylulose <=> D-Fructose	−22
Formaldehyde + D-Ribose <=> D-Glucose	−16
Formaldehyde + D-Ribose <=> D-Fructose	−16
D-Glyceraldehyde + Glycerone phosphate <=> D-Fructose 1-phosphate	−14
Acetaldehyde + Formate <=> L-Lactate	−10
Formaldehyde + D-Ribulose 5-phosphate <=> D-arabino-Hex-3-ulose 6-phosphate	−8
D-Glyceraldehyde + Glyceron = D-Fructose	−7
(S)-Lactaldehyde + Pyruvate <=> 2-Dehydro-3-deoxy-D-fuconate	−5
D-Glyceraldehyde 3-phosphate + Glycerone phosphate <=> D-Fructose 1,6-bisphosphate	−4
Formaldehyde + D-Alanine <=> 2-Methylserine	−4
Formaldehyde + D-Serine <=> 2-Hydroxymethylserine	−4
Acetaldehyde + D-Glyceraldehyde 3-phosphate <=> 2-Deoxy-D-ribose 5-phosphate	−4
(S)-Lactaldehyde + Glycerone phosphate <=> L-Fuculose 1-phosphate	−3
Glycolaldehyde + Pyruvate <=> 2-Dehydro-3-deoxy-L-arabinonate	−3
Formaldehyde + Glycerone phosphate <=> Erythrulose 1-phosphate	−2
D-Glyceraldehyde 3-phosphate + Pyruvate <=> 2-Dehydro-3-deoxy-6-phospho-D-gluconate	−2
Formaldehyde + Acetate <=> 3-Hydroxypropanoate	−1
Glyoxylate + Methanol <=> Glycerate	0
Formaldehyde + Methane <=> Ethanol	0
D-Glyceraldehyde 3-phosphate + Pyruvate <=> 2-Dehydro-3-deoxy-D-galactonate 6-phosphate	1
Glyoxylate + Acetyl-CoA <=> Malyl-CoA	3
Glyoxylate + Pyruvate <=> 4-Hydroxy-2-oxoglutarate	4
Acetaldehyde + Methane <=> Isopropanol	5
Acetaldehyde + Glycine <=> L-Threonine	7
Formaldehyde + Glyoxylate <=> Hydroxypyruvate	8
(S)-Lactaldehyde + Glycerone phosphate <=> L-Rhamnulose 1-phosphate	11
Glyoxylate + Acetate <=> Malate	11
Oxaloacetate + Acetate <=> Citrate	15
Pyruvate + Propanoate <=> (2R,3 S)-2,3-Dimethylmalate	15
Pyruvate + Acetate <=> (S)-2-Methylmalate	15
Formaldehyde + Glycine <=> L-Serine	17
Glyoxylate + Succinate <=> Isocitrate	18
Formaldehyde + Glycolate <=> Glycerate	18
Hydroxycarbon (not methanol) reduction and condensation	
Hydroxypyruvate + Formate <=> Oxaloacetate + H_2O	−55
2 Ethanol <=> Butanol + H_2O	−46
2 Glycolate <=> Malate + H_2O	−2
Glycolate + Malate <=> Isocitrate + H_2O	−5
Glycolate + Malate <=> Citrate + H_2O	−12
Glycolate + Acetate <=> Succinate + H_2O	−12
Glycolate + Glyoxylate <=> Oxaloacetate + H_2O	−15
Glycolate + Acetyl-CoA <=> Succinyl-CoA + H_2O	−19
Methanol reduction and condensation	
Methanol + Acetaldehyde <=> Acetone + H_2O	−66
Methanol + Formate <=> Acetate + H_2O	−63
Methanol + Formaldehyde <=> Acetaldehyde + H_2O	−53
2 Methanol <=> Ethanol + H_2O	−51
Methanol + Ethanol <=> Propanol + H_2O	−39
Methanol + Propanol <=> Butanol + H_2O	−41
Methanol + Glyoxylate <=> Pyruvate + H_2O	−48
Methanol + Glycolate <=> 3-Hydroxypropanoate + H_2O	−32

References

[1] R. Heinrich, S. Schuster, H.G. Holzhutter, Mathematical analysis of enzymic reaction systems using optimization principles, Eur. J. Biochem. 201 (1991) 1–21.
[2] R. Heinrich, H.G. Holzhutter, S. Schuster, A theoretical approach to the evolution and structural design of enzymatic networks: linear enzymatic chains, branched pathways and glycolysis of erythrocytes, Bull. Math. Biol. 49 (1987) 539–595.
[3] E. Melendez-Hevia, T.G. Waddell, R. Heinrich, F. Montero, Theoretical approaches to the evolutionary optimization of glycolysis–chemical analysis, Eur. J. Biochem. 244 (1997) 527–543.
[4] E. Melendez-Hevia, A. Isidoro, The game of the pentose phosphate cycle, J. Theor. Biol. 117 (1985) 251–263.
[5] E. Melendez-Hevia, T.G. Waddell, F. Montero, Optimization of metabolism: the evolution of metabolic pathways toward simplicity through the game of the pentose phosphate cycle, J. Theor. Biol. 166 (1994) 201–219.
[6] E. Melendez-Hevia, T.G. Waddell, M. Cascante, The puzzle of the Krebs citric acid cycle: assembling the pieces of chemically feasible reactions, and opportunism in the design of metabolic pathways during evolution, J. Mol. Evol. 43 (1996) 293–303.
[7] R.K. Thauer, K. Jungermann, K. Decker, Energy conservation in chemotrophic anaerobic bacteria, Bacteriol. Rev. 41 (1977) 100–180.
[8] M.L. Mavrovouniotis, Identification of localized and distributed bottlenecks in metabolic pathways, Proc. Int. Conf. Intell. Syst. Mol. Biol. 1 (1993) 275–283.
[9] B. Schink, Energetics of syntrophic cooperation in methanogenic degradation, Microbiol. Mol. Biol. Rev. 61 (1997) 262–280.
[10] T.J. Erb, Carboxylases in natural and synthetic microbial pathways, Appl. Environ. Microbiol. 77 (2011) 8466–8477.
[11] G. Fuchs, Alternative Pathways of Carbon Dioxide Fixation - Insights into the Early Evolution of Life, Annu. Rev. Microbiol. 65 (2011) 631–658.
[12] A. Bar-Even, E. Noor, R. Milo, A survey of carbon fixation pathways through a quantitative lens, J. Exp. Bot. 63 (2012) 2325–2342.
[13] I.A. Berg, D. Kockelkorn, W.H. Ramos-Vera, R.F. Say, J. Zarzycki, M. Hugler, B.E. Alber, G. Fuchs, Autotrophic carbon fixation in archaea, Nat. Rev. Microbiol. 8 (2010) 447–460.
[14] I.A. Berg, Ecological Aspects of the Distribution of Different Autotrophic CO2 Fixation Pathways, Appl. Environ. Microbiol. 77 (2011) 1925–1936.
[15] C.A. Raines, The Calvin cycle revisited, Photosynth. Res. 75 (2003) 1–10.
[16] C.A. Raines, Transgenic approaches to manipulate the environmental responses of the C3 carbon fixation cycle, Plant Cell Environ. 29 (2006) 331–339.
[17] C. Peterhansel, M. Niessen, R.M. Kebeish, Metabolic engineering towards the enhancement of photosynthesis, Photochem. Photobiol. 84 (2008) 1317–1323.
[18] M. Stitt, D. Schulze, Does Rubisco control the rate of photosynthesis and plant growth? An exercise in molecular ecophysiology, Plant Cell Environ. 17 (1994) 465–487.
[19] M.G. Poolman, D.A. Fell, S. Thomas, Modelling photosynthesis and its control, J. Exp. Bot. 51 Spec No (2000) 319–328.
[20] M. Hugler, S.M. Sievert, Beyond the Calvin cycle: autotrophic carbon fixation in the ocean, Ann. Rev. Mar. Sci. 3 (2011) 261–289.
[21] T. Sato, H. Atomi, Microbial Inorganic Carbon Fixation, Encyclopedia of Life Sciences, 2010.

[22] H.L. Drake, K. Kirsten, C. Matthies, Acetogenic Prokaryotes, The Prokaryotes, Springer, New York, 2006, pp. 354–420.
[23] H.L. Drake, A.S. Gossner, S.L. Daniel, Old acetogens, new light, Ann. N. Y. Acad. Sci. 1125 (2008) 100–128.
[24] S.W. Ragsdale, Enzymology of the wood-Ljungdahl pathway of acetogenesis, Ann. N. Y. Acad. Sci. 1125 (2008) 129–136.
[25] S.W. Ragsdale, E. Pierce, Acetogenesis and the Wood-Ljungdahl pathway of CO(2) fixation, Biochim. Biophys. Acta 1784 (2008) 1873–1898.
[26] L.G. Ljungdahl, The autotrophic pathway of acetate synthesis in acetogenic bacteria, Annu. Rev. Microbiol. 40 (1986) 415–450.
[27] G. Fuchs, CO2 fixation in acetogenic bacteria: variations on a theme, FEMS Microbiol. Lett. 39 (1985) 181–213.
[28] A. Bar-Even, E. Noor, N.E. Lewis, R. Milo, Design and analysis of synthetic carbon fixation pathways, Proc. Natl. Acad. Sci. U. S. A. 107 (2010) 8889–8894.
[29] R.A. Alberty, A. Cornish-Bowden, R.N. Goldberg, G.G. Hammes, K. Tipton, H.V. Westerhoff, Recommendations for terminology and databases for biochemical thermodynamics, Biophys. Chem. 155 (2011) 89–103.
[30] B.D. Bennett, E.H. Kimball, M. Gao, R. Osterhout, S.J. Van Dien, J.D. Rabinowitz, Absolute metabolite concentrations and implied enzyme active site occupancy in Escherichia coli, Nat. Chem. Biol. 5 (2009) 593–599.
[31] C.S. Henry, M.D. Jankowski, L.J. Broadbelt, V. Hatzimanikatis, Genome-scale thermodynamic analysis of Escherichia coli metabolism, Biophys. J. 90 (2006) 1453–1461.
[32] A.L. Weber, Chemical constraints governing the origin of metabolism: the thermodynamic landscape of carbon group transformations under mild aqueous conditions, Orig. Life Evol. Biosph. 32 (2002) 333–357.
[33] A. Bar-Even, E. Noor, A. Flamholz, J.M. Buescher, R. Milo, Hydrophobicity and charge shape cellular metabolite concentrations, PLoS Comput. Biol. 7 (2011) e1002166.
[34] A. Flamholz, E. Noor, A. Bar-Even, R. Milo, eQuilibrator–the biochemical thermodynamics calculator, Nucleic Acids Res. 40 (2012) D770–D775.
[35] R.N. Goldberg, Y.B. Tewari, T.N. Bhat, Thermodynamics of enzyme-catalyzed reactions–a database for quantitative biochemistry, Bioinformatics 20 (2004) 2874–2877.
[36] R.A. Alberty, Thermodynamics of Biochemical Reactions, Wiley-Interscience, 2003.
[37] R.A. Alberty, Calculation of thermodynamic properties of species of biochemical reactants using the inverse Legendre transform, J. Phys. Chem. B 109 (2005) 9132–9139.
[38] R.A. Alberty, Biochemical thermodynamics: applications of Mathematica, Methods Biochem. Anal. 48 (2006) 1–458.
[39] M.D. Jankowski, C.S. Henry, L.J. Broadbelt, V. Hatzimanikatis, Group contribution method for thermodynamic analysis of complex metabolic networks, Biophys. J. 95 (2008) 1487–1499.
[40] J.M. Liegel, The Equilibrium constant for the glycine synthase reaction, University of Texas, 1985.
[41] B.E. Maden, Tetrahydrofolate and tetrahydromethanopterin compared: functionally distinct carriers in C1 metabolism, Biochem. J. 350 (Pt 3) (2000) 609–629.
[42] N. Ishii, K. Nakahigashi, T. Baba, M. Robert, T. Soga, A. Kanai, T. Hirasawa, M. Naba, K. Hirai, A. Hoque, P.Y. Ho, Y. Kakazu, K. Sugawara, S. Igarashi, S. Harada, T. Masuda, N. Sugiyama, T. Togashi, M. Hasegawa, Y. Takai, K. Yugi, K. Arakawa, N. Iwata, Y. Toya, Y. Nakayama, T. Nishioka, K. Shimizu, H. Mori, M. Tomita, Multiple high-throughput analyses monitor the response of E. coli to perturbations, Science 316 (2007) 593–597.
[43] G. Forti, A. Furia, P. Bombelli, G. Finazzi, *In vivo* changes of the oxidation-reduction state of NADP and of the ATP/ADP cellular ratio linked to the photosynthetic activity in Chlamydomonas reinhardtii, Plant Physiol. 132 (2003) 1464–1474.
[44] D. Heineke, B. Riens, H. Grosse, P. Hoferichter, U. Peter, U.I. Flugge, H.W. Heldt, Redox Transfer across the Inner Chloroplast Envelope Membrane, Plant Physiol. 95 (1991) 1131–1137.
[45] K.J. Dietz, U. Heber, Rate-limiting factors in leaf photosynthesis I. carbon fluxes in the calvin cycle, Biochim. Biophys. Acta 767 (1984) 432–443.
[46] E.I. Stiefel, G.N. George, Ferredoxins, Hydrogenases, and Nitrogenases: Metal-Sulfide Proteins, Bioinorganic Chemistry, University Science Books, 1994, pp. 365–453.
[47] R.S. Magliozzo, B.A. McIntosh, W.V. Sweeney, Origin of the pH dependence of the midpoint reduction potential in Clostridium pasteurianum ferredoxin:oxidation state-dependent hydrogen ion association, J. Biol. Chem. 257 (1982) 3506–3509.
[48] R.C. Prince, M.W. Adams, Oxidation-reduction properties of the two Fe4S4 clusters in Clostridium pasteurianum ferredoxin, J. Biol. Chem. 262 (1987) 5125–5128.
[49] L. Calzolai, L. Messori, R. Monnanni, The pH dependent spectral properties of Clostridium pasteurianum 2[Fe4S4] ferredoxin, FEBS Lett. 350 (1994) 41–45.
[50] M.F. Verhagen, T.A. Link, W.R. Hagen, Electrochemical study of the redox properties of [2Fe-2S] ferredoxins. Evidence for superreduction of the Rieske [2Fe-2S] cluster, FEBS Lett. 361 (1995) 75–78.
[51] G. Schneider, Y. Lindqvist, C.I. Branden, RUBISCO: structure and mechanism, Annu. Rev. Biophys. Biomol. Struct. 21 (1992) 119–143.
[52] W.F. Martin, Hydrogen, metals, bifurcating electrons, and proton gradients: The early evolution of biological energy conservation, FEBS Lett. 586 (2012) 485–493.
[53] R. Douce, J. Bourguignon, M. Neuburger, F. Rebeille, The glycine decarboxylase system: a fascinating complex, Trends Plant Sci. 6 (2001) 167–176.
[54] A. He, T. Li, L. Daniels, I. Fotheringham, J.P. Rosazza, Nocardia sp. carboxylic acid reductase: cloning, expression, and characterization of a new aldehyde oxidoreductase family, Appl. Environ. Microbiol. 70 (2004) 1874–1881.
[55] T. Li, J.P. Rosazza, Purification, characterization, and properties of an aryl aldehyde oxidoreductase from Nocardia sp. strain NRRL 5646, J. Bacteriol. 179 (1997) 3482–3487.
[56] P. Venkitasubramanian, L. Daniels, J.P. Rosazza, Reduction of carboxylic acids by Nocardia aldehyde oxidoreductase requires a phosphopantetheinylated enzyme, J. Biol. Chem. 282 (2007) 478–485.
[57] A. Bar-Even, E. Noor, Y. Savir, W. Liebermeister, D. Davidi, D.S. Tawfik, R. Milo, The moderately efficient enzyme: evolutionary and physicochemical trends shaping enzyme parameters, Biochemistry 50 (2011) 4402–4410.
[58] L. Stols, M.I. Donnelly, Production of succinic acid through overexpression of NAD(+)-dependent malic enzyme in an Escherichia coli mutant, Appl. Environ. Microbiol. 63 (1997) 2695–2701.
[59] M. Cocaign-Bousquet, A. Guyonvarch, N.D. Lindley, Growth Rate-Dependent Modulation of Carbon Flux through Central Metabolism and the Kinetic Consequences for Glucose-Limited Chemostat Cultures of Corynebacterium glutamicum, Appl. Environ. Microbiol. 62 (1996) 429–436.
[60] R.M. Zelle, J.C. Harrison, J.T. Pronk, A.J. van Maris, Anaplerotic role for cytosolic malic enzyme in engineered Saccharomyces cerevisiae strains, Appl. Environ. Microbiol. 77 (2011) 732–738.
[61] K.M. Pound, N. Sorokina, K. Ballal, D.A. Berkich, M. Fasano, K.F. Lanoue, H. Taegtmeyer, J.M. O'Donnell, E.D. Lewandowski, Substrate-enzyme competition attenuates upregulated anaplerotic flux through malic enzyme in hypertrophied rat heart and restores triacylglyceride content: attenuating upregulated anaplerosis in hypertrophy, Circ. Res. 104 (2009) 805–812.
[62] K.E. Sundqvist, J. Heikkila, I.E. Hassinen, J.K. Hiltunen, Role of NADP+ (corrected)-linked malic enzymes as regulators of the pool size of tricarboxylic acid-cycle intermediates in the perfused rat heart, Biochem. J. 243 (1987) 853–857.
[63] T.J. Erb, V. Brecht, G. Fuchs, M. Muller, B.E. Alber, Carboxylation mechanism and stereochemistry of crotonyl-CoA carboxylase/reductase, a carboxylating enoyl-thioester reductase, Proc. Natl. Acad. Sci. U. S. A. 106 (2009) 8871–8876.
[64] N. Quade, L. Huo, S. Rachid, D.W. Heinz, R. Muller, Unusual carbon fixation gives rise to diverse polyketide extender units, Nat. Chem. Biol. 8 (2012) 117–124.
[65] B.S.J. Winkel, Metabolic Channeling in Plants, Annu. Rev. Plant Biol. 55 (2004) 85–107.
[66] C.L. Liu, N. Hart, H.D. Peck Jr., Inorganic pyrophosphate: energy source for sulfate-reducing bacteria of the genus desulfotomaculum, Science 217 (1982) 363–364.
[67] M. Baltscheffsky, Inorganic pyrophosphate and ATP as energy donors in chromatophores from Rhodospirillum rubrum, Nature 216 (1967) 241–243.
[68] L. de Meis, Pyrophosphate of high and low energy. Contributions of pH, Ca2+, Mg2+, and water to free energy of hydrolysis, J. Biol. Chem. 259 (1984) 6090–6097.
[69] H.G. Wood, Some reactions in which inorganic pyrophosphate replaces ATP and serves as a source of energy, Fed. Proc. 36 (1977) 2197–2206.
[70] J.R. Perez-Castineira, R. Gomez-Garcia, R.L. Lopez-Marques, M. Losada, A. Serrano, Enzymatic systems of inorganic pyrophosphate bioenergetics in photosynthetic and heterotrophic protists: remnants or metabolic cornerstones? Int. Microbiol. 4 (2001) 135–142.
[71] A. Chi, R.G. Kemp, The primordial high energy compound: ATP or inorganic pyrophosphate? J. Biol. Chem. 275 (2000) 35677–35679.
[72] A. Finkelstein, Water and nonelectrolyte permeability of lipid bilayer membranes, J. Gen. Physiol. 68 (1976) 127–135.
[73] S. Winiwarter, N.M. Bonham, F. Ax, A. Hallberg, H. Lennernas, A. Karlen, Correlation of human jejunal permeability (*in vivo*) of drugs with experimentally and theoretically derived parameters. A multivariate data analysis approach, J. Med. Chem. 41 (1998) 4939–4949.
[74] A.C. Chakrabarti, D.W. Deamer, Permeation of membranes by the neutral form of amino acids and peptides: relevance to the origin of peptide translocation, J. Mol. Evol. 39 (1994) 1–5.
[75] B.D. Davis, On the importance of being ionized, Arch. Biochem. Biophys. 78 (1958) 497–509.
[76] F.H. Westheimer, Why nature chose phosphates, Science 235 (1987) 1173–1178.
[77] S. Estelmann, M. Hugler, W. Eisenreich, K. Werner, I.A. Berg, W.H. Ramos-Vera, R.F. Say, D. Kockelkorn, N. Gad'on, G. Fuchs, Labeling and enzyme studies of the central carbon metabolism in Metallosphaera sedula, J. Bacteriol. 193 (2011) 1191–1200.